

## Analysis of deformations in soft clay due to unloading

*Master of Science Thesis in the Master's Programme Geo and Water Engineering*

ARAZ ISMAIL  
FITSUM TESHOME

Department of Civil and Environmental Engineering  
*Division of GeoEngineering*

*Geotechnical Engineering Research Group*

CHALMERS UNIVERSITY OF TECHNOLOGY  
Goteborg, Sweden 2011  
Master's Thesis 2011:23



MASTER'S THESIS 2011:23

# Analysis of deformations in soft clay due to unloading

*Master of Science Thesis in the Master's Programme Geo and Water Engineering*

ARAZ ISMAIL

FITSUM TESHOME

Department of Civil and Environmental Engineering

*Division of GeoEngineering*

*Geotechnical Engineering Research Group*

CHALMERS UNIVERSITY OF TECHNOLOGY

Göteborg, Sweden 2011

Analysis of deformations in soft clay due to unloading  
*Master of Science Thesis in the Master's Programme Geo and Water Engineering*  
ARAZ ISMAIL  
FITSUM TESHOME

© ARAZ ISMAIL & FITSUM TESHOME, 2011

Examensarbete / Institutionen för bygg- och miljöteknik,  
Chalmers tekniska högskola 2011:23

Department of Civil and Environmental Engineering  
Division of GeoEngineering  
Geotechnical Engineering Research Group  
Chalmers University of Technology  
SE-412 96 Göteborg  
Sweden  
Telephone: + 46 (0)31-772 1000

Cover: Excavation under the bridge at section E13 at Lärjeholm and horizontal displacement readings in contour form in Plaxis. The picture was taken by Fitsum Teshome in January 2011.

Chalmers Reproservice  
Göteborg, Sweden 2011

Analysis of deformations in soft clay due to unloading  
*Master of Science Thesis in the Master's Programme Geo and Water Engineering*

ARAZ ISMAIL

FITSUM TESHOME

Department of Civil and Environmental Engineering

Division of GeoEngineering

Geotechnical Engineering Research Group

Chalmers University of Technology

## ABSTRACT

In infrastructure projects such as road and railway construction it is necessary to perform a number of earth excavations wherever required. These excavations cause difficulties regarding deformations and slope stability on the soil mass. The deformation of soil is highly dependent on the stiffness of the soil. Therefore, it is of particular interest to determine the appropriate stiffness modulus of soil in order to study the deformation properties of soil. The objective of this thesis is to study in depth the deformation of soft clay due to unloading or excavation.

In this project the excavation was carried out on section E13 at Lärjeholm which is part of the undergoing new railway project between Gothenburg and Trollhättan. It was carried out on soil layer that consisted of silty sand for the first few meters and soft clay for deep layers below. Due to the construction conditions of the area, the excavation was taking place under the newly constructed bridge and the existing highway E45 near this section had to be diverted and placed under this bridge. This thesis focuses on the deformation analysis of soft clay due to this excavation. The deformation analysis mainly deals with the unloading modulus based on field deformation measurements, field and laboratory tests and previously conducted research on the unloading modulus of soft clay.

The field deformation measurements were taken from an inclinometer device, surface point measurements and bridge point measurements installed at different location where the excavation is taking place. The laboratory tests mainly include the oedometer, CRS test where the two different soil stiffness moduli,  $M_0$  and  $M_L$  are obtained. However, in this case, due to unloading and the clay being slightly over consolidated, the modulus  $M_0$  was only considered.

In this thesis, the main deformation analysis was performed through the help of the finite element based geotechnical computer software called Plaxis. For the simulation, two soil models, namely; Mohr coulomb and Hardening soil, were used in order to catch the real deformation behaviour of soft clay. The results of the analysis from these soil models are cross checked with the field deformation measurements and the unloading modulus is estimated through back calculation. Based on this, a conclusion is made to verify which approach gives a reasonable and realistic unloading modulus.

Key words: Clay, excavation, deformations, unloading modulus

# Contents

ABSTRACT	I
CONTENTS	II
PREFACE	IV
NOTATIONS	V
1. INTRODUCTION	1
1.1 Background	2
1.2 Aim	3
1.3 Material and method	3
1.4 Delimitation	3
2. THEORY	4
2.1 Properties of soil	4
2.1.1 Density	5
2.1.2 Porosity	6
2.1.3 Consistency limits	6
2.1.4 Natural water content	8
2.1.5 Shear strength (Vane, cone, CPT, shear test)	8
2.1.6 Sensitivity	9
2.1.7 Effective stress and pre-consolidation pressure	9
2.1.7 Permeability	10
2.2 Deformation of soft soil	10
2.2.1 Soil stiffness	11
2.2.2 Unloading modulus	12
2.2.3 Deformation determination	13
2.3 Empirics	16
2.3.1 Shear strength	16
2.3.2 Modulus	17
2.4 Plaxis	18
2.4.1 Input	18
2.4.2 Calculation	19
2.4.3 Output	19
2.4.4 Soil models	20
3. DEFORMATIONS ANALYSIS OF SECTION E13	25
3.1 Area description	25
3.2 Topography	25
3.3 Pore water pressure	25
3.4 Soil profile	26
3.5 Soil parameters	26

3.5.1 Density	26
3.5.2 Water content	27
3.5.3 Liquid limit	28
3.5.4 Sensitivity	29
3.5.5 Shear strength	30
3.5.6 Effective stresses and pre-consolidation pressure	32
3.5.7 Permeability	32
3.5.8 Stiffness modulus	33
3.6 Excavation procedure	34
3.7 Deformation measurement	35
3.7.1 Inclinator readings	37
3.7.2 Gauges readings	38
4. PLAXIS ANALYSIS	41
4.1 Input phase	41
4.1.1 Mohr coulomb	42
4.1.2 Hardening soil	44
4.2 Calculation phase	46
4.3 Outputs	47
4.3.1 Mohr coulomb	48
4.3.1 Hardening soil	49
5. RESULT COMPARISON	53
6. PARAMETER ANALYSIS	55
7. CONCLUSION AND DISCUSSION	57
8. RECOMMENDATIONS	58
REFERENCES	59
APPENDICES	61

## Preface

The work presented in this paper was executed as part of technical analysis of deformation of soft clay at Norconsult and as a master's thesis for the program Geo and Water Engineering at the division of Geo-Engineering at Chalmers University of Technology. The thesis was conducted for five months, from January 2011 to May 2011.

First of all, we would like to thank our examiner Professor Claes Alén for not only giving us this precious opportunity to work on the master's thesis on an ongoing real project but also for the wonderful lectures he provided in different courses in the masters program.

The next acknowledgement directly goes to our main supervisor Bernhard Gervide Eckel, who was responsible for this master's thesis at Norconsult. Without his excellent academic guidance, material support and interesting technical and social discussions this thesis would never had become reality.

We would like to express our gratitude to Anders Kullingsjö, who was the supervisor at Chalmers side. We are very grateful for his support regarding the basic concepts behind the deformations of soft clay and the sophisticated geotechnical computer software Plaxis.

We would like to thank staffs at Norconsult office for their technical and material support. Special thanks go to Daniel Svärd, who helped us with geotechnical issues, and offices formalities that we were not aware of, and Walter Gabrijelcic, for his assistance regarding field measurements including the inclinometer device, during our site visit in the actual excavation area.

Last but not least, we would like to thank our families for their never-ending support and encouragement not only with the master's thesis but also throughout our academic progressions.



## Notations

### Roman upper case letters

$V_s$	Particle (substance) volume
$V_p$	Pore volume
$V_{tot}$	Total sample volume
$W_p$	Plastic limit
$W_L$	Liquid limit
$W_n$	Water content
$S_i$	Sensitivity
$OCR$	Over-consolidation ratio
$POP$	Pre-over burden pressure
$M_u$	Unloading modulus
$M_r$	Reloading modulus
$M_s$	Secant modulus
$M_t$	Tangent modulus
$M_c$	Cyclic modulus
$M_0$	Elastic modulus
$M_L$	Plastic modulus
$c_v$	Coefficient of consolidation
$c_{uk}$	Undrained shear strength
$c$	Cohesion, shear strength
$E_{oed}$	Plastic modulus
$E_{50}$	Secant modulus
$E_{ur}$	Unloading modulus
$E$	Elastic modulus (Young`s modulus)
$E^`$	Effective elastic modulus (Effective Young`s modulus)
$F$	Safety factor
$p^{ref}$	Reference stress

### Roman lower case letters

$n$	Porosity
$m$	Mass of soil
$ms$	Mass of substance
$e$	Void ratio
$m_w$	Mass of water
$k$	Permeability
$u$	Pore water pressure

### Greek letters

$\rho$	Bulk density
$\rho_s$	Compact density
$\tau_{fu}$	Reduced undrained shear strength
$\mu$	Correction factor
$\tau_{fk}$	Unreduced shear strength

$\tau_{rem}$	Remoulded shear strength
$\sigma$	Total stresses
$\sigma'$	Effective stresses
$\varepsilon$	Strains
$\sigma'_c$	Over-consolidation pressure
$\nu$	Poisons ratio
$\varphi$	Friction angle
$\Psi$	Dilatancy angle
$\sigma_1$	Major principal stress
$\sigma_3$	Minor principal stress

# 1. Introduction

A new railway project that connects Gothenburg and Trollhättan is under way; involving Swedish road administration, Trafikverket, as a client and constructed by different contractors that are involved in the project. This thesis focuses on section E13 at Lärjeholm, which is located north of Gothenburg city. This section is constructed by Veidekke entreprenad AB and involves the construction of two new railways along the existing railway, which is adjacent to E45, see Figure 1.



Figure 1: Location of section E13 at Lärjeholm. (Eniro, 2011)

The construction of the two bridges for the railways crosses the existing highway, E45. Due to this, the existing highway, E45, will be diverted and placed under one of the railway bridges, see Figure 2. This involves excavation under one of the two bridges that is already constructed. The excavation in the area will cause considerable deformations in soft clay soil where the bridges and their foundation rest on. These deformations will cause a movement on the bridge foundations in direction of the excavation, especially at one end where the bridge support system is a hinge type.

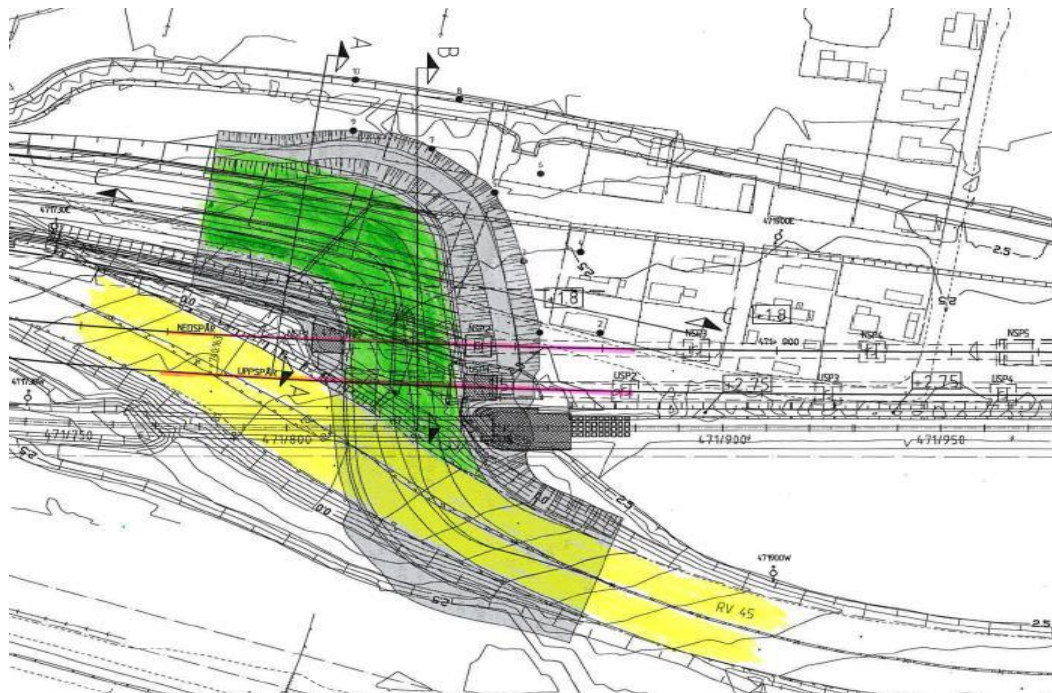


Figure 2: Detail section of E13, which consists of the existing highway marked in yellow, the two railway bridges, USP and NSP, marked in red, and the excavation area marked in green.

During this temporary traffic stage under one of the bridges deformation measurements were executed. Based on these measurements and with full scale excavation test and its evaluation the deformation properties of the soil were developed. In this thesis, this deformation analysis of soft clay due to the excavation is performed with the help of geotechnical software called Plaxis. The results from field deformation measurements and Plaxis deformation analysis are also compared in order to achieve better results regarding the deformation properties of soft clay soil. Moreover, predictions on the deformations that are expected to occur in the next main excavation stage near section E13 can be made based on the deformation analysis of soft clay at section E13 at Lärjeholm.

## 1.1 Background

The new rail way project between Gothenburg and Trollhättan involves the construction of two new railway bridges namely USP and NSP, at section E13 at Lärjeholm. Due to the conditions in the construction area, the existing highway E45 must be temporarily diverted and placed under one of the two new bridges. However this process involves excavation under the bridges. The excavation includes removal of six meters of soil that consists of silty-sand for the first two meters and soft clay for the other four meters. As consequence of this excavation, horizontal and vertical deformations are expected.

To evaluate the deformations due to this excavation, Norconsult will perform field and technical deformation analysis. The field analysis is performed by installing inclinometer and point measurement devices at the actual excavation area, where these devices measure the deformations at the different stages of the excavation. The technical analysis involves usage of geotechnical software to simulate the deformation due to this excavation. This thesis is part of the technical deformation analysis where Plaxis, a finite element based advanced geotechnical software is used for the

deformation simulation. The simulation in thesis is performed by using field and laboratory data of soil parameters of the excavation area and by using these parameter values as an input for Plaxis and interpreting the output values. In the simulation two different soil models are used, namely Mohr coulomb and hardening soil model in order to take into account the mechanical deformation properties of soil and obtain a better and realistic result from the analysis. The outputs from Plaxis deformation simulation is compared with results from the field measurements in order to control the different soil parameters and empirical approaches used in the analysis. Furthermore, parameter analysis is performed to see which soil parameter and factor has significant influence on the deformation of soft clay. Finally, conclusions and recommendations are made on the deformation of soft soil due to unloading based the field and technical deformation analysis.

## **1.2 Aim**

The aim of this project is to study in depth the deformation properties of soft clay due to excavation, and to use this analysis as a basis to decide which soil parameter has substantial influence on the deformation of soft clay. Special attention is given to the stiffness Modulus that will contribute much in the deformation analysis and computer simulation. This is because, in this case, due to unloading of the soil, the stiffness modulus is expected to be different from the one that is obtained from the oedometer or triaxial laboratory test. Different empirical approaches are used to get a reasonable and accurate unloading modulus. Furthermore, measurement readings of deformation on the site are compared with output from plaxis software simulation to see which empirical approach gives better and realistic result.

## **1.3 Material and method**

In this project different materials such as geotechnics compendium, lecture notes from infrastructural geo engineering course, different internet sources, and different geotechnical reading materials that are available as softcopy and hard copy at norconsult are used. Moreover borehole data from the site and Plaxis computer program are used for the deformation analysis.

## **1.4 Delimitation**

Section E13 at Lärjeholm or the excavation area under the bridge, where the existing E45 will be diverted and placed under the bridge, is the area where this thesis mainly focuses on. Only this section will be discussed in this project, and prediction on the other excavations will be made based upon the analysis in this section.

## 2. Theory

In this chapter, basic theories and literature reviews that are relevant to this thesis are presented. The basic theories behind the deformation properties of soil, field and laboratory tests are discussed. The empirical approaches that available to control investigated soil parameters are also discussed. Finally, some concepts about Plaxis, software used for deformation analysis, are discussed.

### 2.1 Properties of soil

The loose part of the earth's crust consists of different soil types, for instance, sand, till and clay. These different types of soils are made up of two different kinds of components, particles and pores. The pores are filled with water or gas or both, see Figure 3. The relationships between the volumes of all these different parts have a great impact on the geo-technical properties of a soil, such as density, porosity, water ratio. (Larsson, 2008)

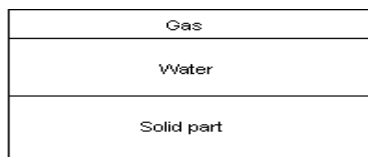


Figure 3: The relation between particles and pores.

Other important factors having a major impact on the properties of a soil are the shape of the particles and the distribution of the size of the grains. These factors affect the geo-technical properties of a soil, such as strength, deformation, capillarity and permeability properties.

Clay, which is considered as a soft soil, is very common soil in south-western part of Sweden. Clay has a grain size less than 0.002 mm, which is a low value when compared to the grain size of sand, which has a size between 0.06-2 mm, see Figure 4.

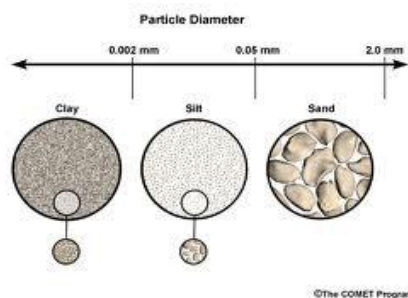


Figure 4: Grain size of clay, silt and sand. (The COMET program, 2011)

Due to the size of the grains of clay and its poor contact with each other, clay has lower permeability and strength and lower deformation resistance than a soil with bigger grains like sand. The particles in clay are not in direct contact with each other when compared to other soils consisting of bigger particles. Instead the particles in clay are adhered together by molecular attraction forces. This means that clay has an open structure that makes it to be very compressible soil, see Figure 5. (Sällfors, 2001)

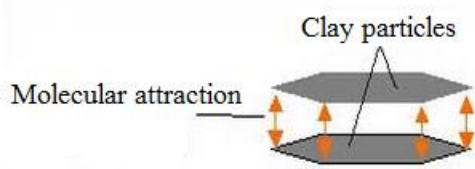


Figure 5: Molecular attraction between clay particles. (SGI, 1995)

Clay that has been exposed to very high pressures attains a dense structure and makes the clay to be a lower compressible soil than it was before.

When excavating in a clay layer, horizontal and vertical (heave) deformations will occur. Because of this problem, there is a challenge to construct buildings, roads, bridges and railways on a ground with deep layers of clay. Installation of piles and sheet piles and slope stability measures are performed as geotechnical solutions in order to obtain stable excavations and firm foundation, when building bridges, buildings, railways and roads in an area consisting of deep layers of soft clay. (Sällfors, 2001)

### 2.1.1 Density

Density of soils, which represents the physical conditions of soil, is an important parameter that has to be determined, since the value is different for different soil types. Density of soils refers to the mass of small particles that constitutes the soil mass divided by the total volume they occupy. In geotechnical laboratory test, two types of densities are determined; bulk density and compact density, see Table 1 for soil densities of different soil types.

The first one refers to the density of the soil measured including the pores that are contained in the undisturbed soil sample. It is explained in equation (1) below.

$$\rho = \frac{m}{v} \quad (1)$$

Where,  $\rho$  - Bulk density

$m$  - Mass of soil (particles + pores)

$v$  - Total volume

Table 1: Bulk density for some ordinary soil types.

Soil type	Bulk density (t/m <sub>3</sub> )		
	Water saturated	Effective	Un-saturated
Sand	2.1	1.0 - 1.1	1.8
Gravel	2.2	1.1	1.9
Silt	1.9	0.9	1.7
Clay	1.5 - 1.7	0.5 - 0.7	1.6

Meanwhile, the latter density refers to the density of the particles, which is the mass of the substance divided by the volume of the substance. See equation (2) below.

$$\rho_s = \frac{m_s}{v_s} \quad (2)$$

Where,  $\rho_s$  - Compact density

$m_s$  - Mass of substance (particles)

$v_s$  - Volume of substance

### 2.1.2 Porosity

A soil consists of particles and pores, which are filled with water or/and gas as stated in the introduction of this chapter. Porosity of soils,  $n$  is determined by dividing the volume of the pores in a soil sample with the total volume of the soil sample, see equation (3) below.

$$n = \frac{v_p}{v_{tot}} \quad (3)$$

Where,  $n$  - Porosity

$V_p$  - Pore volume

$V_{tot}$  - Total sample volume

The relation between the volume of the pores and the volume of the particles (solid part of the soil) can be seen in equation (4).

$$e = \frac{v_p}{v_s} \quad (4)$$

Where,  $e$  - Pore ratio

$V_p$  - Pore volume

$V_s$  - Particle (substance) volume

The upper two equations can be combined and equation (5) shows the relation.

$$e = \frac{n}{1-n} \quad (5)$$

### 2.1.3 Consistency limits

The consistency in a clay sample is strongly dependent on the water content. The consistency can be plastic, liquid etc. Figure 6 shows the borders between different consistency limits, also called Atterberg's limits of soils.



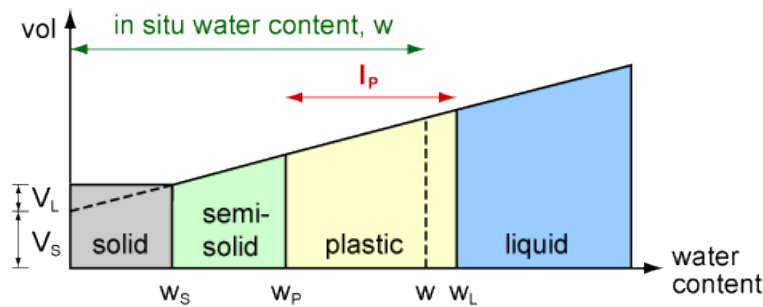


Figure 6: Atterberg's limits, consistency borders for cohesive soil. (GEOTip, 2011)

The liquid limit,  $W_L$  and the plastic limit,  $W_p$  indicate the water content where a cohesive soil sample has a non-plastic, plastic or liquid consistency.

The fall cone test is a Geotechnical laboratory test that is used worldwide, to determine the consistency limits or Atterberg's limits of soils. Among the consistency limits, liquid limit is the parameter determined from this test. Liquid limit is the measure of the water content of clay, at which the soil starts to change from plastic to liquid state. It is expressed in percent, with values in range between 15 and 100%, where this value becomes high up to 90% for highly plastic clay. Even if, liquid limit is one parameter that is determined from the fall cone test, undrained shear strength of the soil at the measured liquid limit is the significant parameter to be evaluated, which then will be used together with the undrained shear strength obtained from field investigation, to determine the actual undrained shear strength of the soil. (Houlsby, 1982)

For this test a piston soil sample is taken in the field, where these samples are taken to the laboratory using ordinary laboratory tubes. The test is performed on undisturbed sample for every meter until certain depth, usually up to 10m, then every two or three meters for the rest of the investigation depth. The cone used in this test has a weight of 10, 60, 100 or 400 gram, with an angle of 30 or 60 degrees at the tip, and it is dropped under controlled conditions on the placed clay sample that has a smooth contact surface. Then the tip of cone starts to penetrate the clay sample, and this procedure will be performed three times. After each test, part of the clay sample which is equal to 1.5 times of the penetration depth is removed and put in a bowl after each step. Finally the average of the three values is evaluated and will be considered as the undrained shear strength of the clay. Another test, but with the same procedure, is performed on a remoulded clay sample, which was the removed clay and put in a bowl during the earlier test. After evaluating the shear strength from this test as well, sensitivity analysis can be performed by comparing the shear strength from the two tests, which will be more explained later under the sensitivity analysis. The device used to perform this test is shown in Figure 7. (Sällfors, 2001)



Figure 7: Measuring equipment for fall cone test (Houlsby, 1982)

A correction factor  $\mu$ , which is a function of liquid limit, see equation (6), will be applied in order to reduce the undrained shear strength obtained from the fall cone test, since the values obtained from the test has shown to be higher than the actual undrained shear strength of the clay.

$$\tau_{fu} = \mu * \tau_{fk} \quad (6)$$

Where,  $\tau_{fu}$  - Corrected undrained shear strength, same as  $c_{uk}$

$$\mu - \text{Correction factor} = (0.43/W_L)^{0.45}$$

$\tau_{fk}$  - Uncorrected shear strength from fall cone test

### 2.1.4 Natural water content

In soil mechanics, natural water content refers to the quantity of water that is found in a given soil sample. It is expressed as the ratio between the weights of water in the soil to the weight of the solid soil, see equation (7).

$$W_n = \frac{m_w}{m_s} \quad (7)$$

Where,  $w_n$  - Water content

$m_w$  - Mass of water

$m_s$  - Mass of solid soil (substance)

### 2.1.5 Shear strength (Vane, cone, CPT, shear test)

Shear strength of soil refers to shear resistance of soil to certain magnitude of shear stress. The shear strength of soil depends on many factors. One factor is soil composition, which refers to the mineralogy, grain size distribution and shape of particles of the soil mass. Additionally, the structure or arrangement of particles of soil layers and joints affects the shear resistance of the soil. Another factor is the initial soil state of the soil, which refers to the stress history of the soil that the soil has been subjected to. Normally there are two ways of modelling the shear strength,

namely as undrained and drained shear strength. The first one refers to the shear strength obtained from soil that passed undrained stress path where water was not allowed to flow into or out of the soil. Meanwhile, the latter one applies to shear strength of soil at which either no water exists or the pore water pressure dissipates during the shearing action.

The shear strength of soil is evaluated by performing field and laboratory tests. Cone penetration test and vane shear tests are in-situ tests where tip and skin resistance of the soil when subjected to loading from devices are measured and converted to shear strength value through empirical correlation. Direct shear test, a laboratory test, is also another test to determine the shear strength of a soil. The test is performed in such a way that undisturbed soil sample is placed inside a shear box and shear force at a confining vertical pressure is applied until the soil sample fails. Stress-strain curves are collected at different intervals for the confining pressure. The rate of strain is varied in order to take into account undrained and drained conditions. Shear strength parameters cohesion ( $c$ ) and internal angle of friction ( $\phi$ ) are evaluated at failure.

### 2.1.6 Sensitivity

Sensitivity test is performed in soft plastic soils that are expected to show a significant reduction of shear strength when subjected to shearing action. As stated earlier, sensitivity test is carried out during fall cone test, and it is defined by the ratio of the undisturbed shear strength divided by the remoulded shear strength, see equation (8) below. (Sällfors, 2001)

$$S_t = \tau_{fu} / \tau_{rem} \quad (8)$$

Where,  $S_t$  - Sensitivity

$\tau_{fu}$  - Undisturbed shear strength

$\tau_{rem}$  - Remoulded shear strength

### 2.1.7 Effective stress and pre-consolidation pressure

The total stress in the soil is a function of the stress transmitted by the soil particles and the water. The constituent of the total stress carried by the soil particles is called effective stress,  $\sigma'$  and the other constituent is called pore water pressure or pore pressure,  $u$  see equation (9). The values of these stress components are evaluated by plotting the accumulated unit weight of the soil and unit weight of water as a function of depth.

$$\sigma = \sigma' + u \quad (9)$$

Where,  $\sigma$  - Total stress

$\sigma'$  - Effective stress

$u$  - Pore water pressure

The pre-consolidation pressure refers to the maximum vertical stress that the soil has been subjected in the past. This parameter is determined from the oedometer laboratory test. It is the breaking point in the stress strain plot obtained from this test. The tangent lines drawn in this bi-linear curve intersect at a point forming an isosceles

triangle and the left corner of this triangle represents the pre-consolidation pressure, see Figure 8. (Sällfors, 2001)

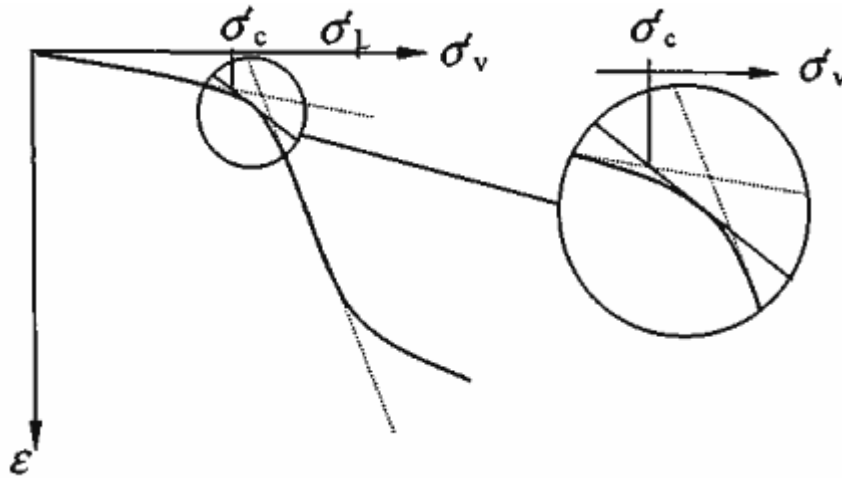


Figure 8: Determination of pre-consolidation pressure. (Persson, 2004)

The relation between the effective stress and the pre-consolidation is expressed as over-consolidation ratio (OCR), which is the ratio between the pre-consolidation and the effective stress, and also as pre-over burden pressure (POP), which is the difference between them. For normally consolidated soils the OCR value is 1 and the POP is 0. These values increase for slightly and heavily over consolidated soils accordingly.

## 2.1.7 Permeability

Permeability ( $k$ ) or sometimes called hydraulic conductivity is the measure of the ability of water to flow through a soil media. It has a measurement unit of m/s. Like other soil parameters permeability of soil is dependent on the soil origin, particle size and distribution and the bond between particles. For instance, the permeability of gravel is higher than sand, and the permeability of sand is higher than silt and clay. Among the listed soil types clay has low permeability due to the above mentioned reason. Usually permeability of soil is determined from laboratory tests known as constant head or falling head permeability test, or sometimes from field test called percolation test. CRS-tests are the most common test in Sweden to determine permeability for clay.

## 2.2 Deformation of soft soil

When a soil is exposed to a certain amount of load it tends to deform in the direction of the application of the load. The type and value of deformation differs from one soil type to another. For instance, soft soil tends to deform in a different manner when compared to stiff soil through application of the same amount of load. The deformation property of soil is dependent on the origin of the soil, the structure of the soil particles, the bond between particles, water content and so on.

In reality, soft soil tends to show nonlinear, plastic and anisotropic deformation behavior. However, different studies conducted on soft soil on the deformation properties or on the stress-strain relationship analysis assume the soil to have linear,

elastic and isotropic deformation behavior, see figure 9. This is due to the fact that the theory of elasticity is intense and easy to apply.

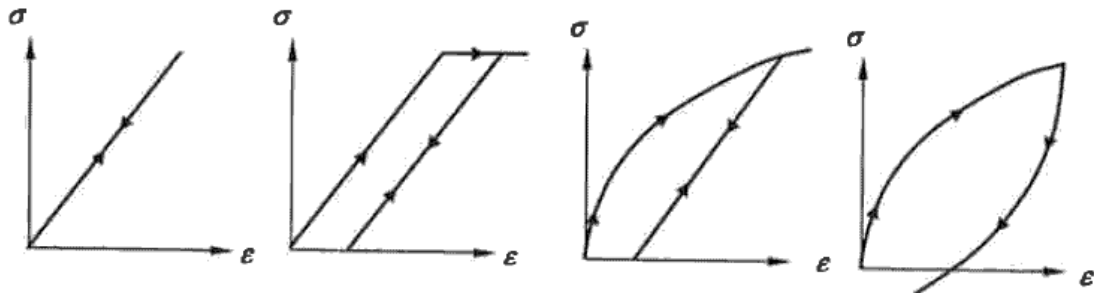


Figure 9: Different material models of soil behaviour: 1) linear elastic model, 2) elastic-perfectly plastic model, 3) non-linear model, 4) elasto-plastic model. (Persson, 2004)

In analysis of deformation of soft soil, the elastic deformation limit is the pre-consolidation or similar yield stress for drained conditions, and shear strength for undrained conditions. Failure criterion is based up on Mohr – coulomb failure criterion, which is determined by performing triaxial and oedometer laboratory tests.

### 2.2.1 Soil stiffness

The stiffness of soil is characterized by the modulus of elasticity or the so called Young’s modulus. This stiffness parameter is usually determined from stress-strain curve obtained from oedometer and triaxial test. The modulus depends on how the particles of the soil are packed and organized. Soil with closely packed particles tends to have a higher modulus value than a soil with particles not closely packed. Water content of the soil also affects the value of modulus. Normally, low water content in the soil leads to high soil modulus. This is due to the fact that at low water content the water binds the particles and thus increases the effective stress among particles through suction. Last but not least, the soil modulus depends on the pre-consolidation pressure, which refers to the pressure or stress that the soil has been subjected to in the past. Normally consolidated soils have lower soil modulus than over consolidated soil. (Briaud, 2010)

To determine the value of the modulus, first, the slope from the curve is evaluated and afterwards the modulus is calculated using empirical formulas, see Figure 10.

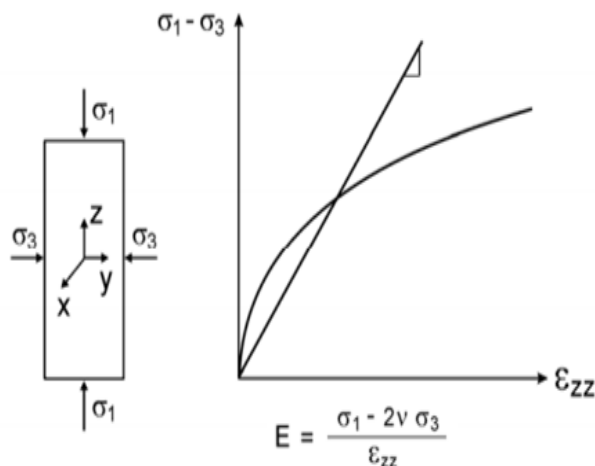


Figure 10: Calculation of modulus of elasticity. (Briaud, 2010)

But different types of modulus are evaluated depending on the properties and conditions of the geotechnical application. These modulus types include secant, tangent, unloading, reloading and cyclic, see Figure 11. The application of these types modulus differs from one geotechnical application to another. For instance, one can use the secant modulus  $M_s$ , in case of strip foundations, to estimate the movement as a result of the application of the load, and one can use the tangent modulus  $M_t$ , to estimate the incremental movement as a result of incremental loading. The unloading modulus  $M_u$ , can be used in excavation analysis when dealing with deformation and heave at the bottom of an excavation, which is the case in this thesis. Furthermore, the reloading modulus  $M_r$  can be used to deal with the movement at the bottom of the excavation when the excavated soil is placed back. Finally, one can use the cyclic modulus  $M_c$ , of soil for analysis of movement in the soil in pile foundation subjected to repeated wave loading.

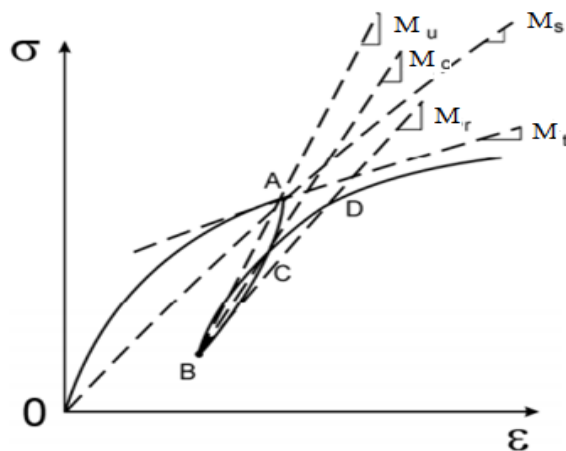


Figure 11: Different types of modulus,  $M_u$ -unloading modulus,  $M_c$ -cyclic modulus,  $M_s$ -secant modulus,  $M_r$ -reloading modulus and  $M_t$ -tangent modulus. (Briaud, 2010)

### 2.2.2 Unloading modulus

As discussed earlier, this thesis deals with the unloading modulus  $M_u$ , since in this case the deformation analysis of clay is carried out under the excavation work. The stress in the clay layer beneath the bottom of the excavation decreases due to unloading. Therefore, the unloading modulus tends to decrease through the depth of an excavation due to considerable decrease of stress. But, due to the effect of creep, the unloading modulus tends to have a large initial value and decreases with the depth of excavation. This is the case especially for normally to slightly consolidated clay, which is the case in this project. (Persson, 2004)

To determine this unloading modulus, unloading and reloading tests have to be carried out. However, in this project these tests are not performed. Instead, unloading modulus values from empirical approaches suggested by different researchers are used as input value in Plaxis for the deformation analysis. Afterwards, the deformation output results from Plaxis are cross checked with the inclinometer deformation readings obtained from the actual excavation area. This method is used as back calculation to determine which empirical approach used in plaxis simulation will give the same result with the inclinometer deformation readings. The different empirical approaches and the outputs from Plaxis simulation are discussed later.

Furthermore, the comparison made between the outputs from Plaxis and inclinometer readings to determine the actual unloading modulus is also presented.

### **2.2.3 Deformation determination**

The deformation of soil is determined by performing laboratory tests by using soil samples collected from the field and by direct measurements in the field where the construction is taking place. The laboratory tests include the oedometer test and triaxial test, and the direct measurements are carried out by using devices such as inclinometer and gauges of timber. The procedures used in these deformation determination methods are discussed below.

#### **2.2.3.1 Oedometer test**

In geotechnical laboratory test program, the oedometer test is the common test performed to determine the deformation properties, consolidation and swelling parameters of soil. It involves two types of methods, namely, incremental load steps and constant rate of strain, CRS. However, in Sweden the constant rate of strain is more often used.

In this constant rate of strain test, CRS, different parameters of a cohesive soil are determined. These parameters include, the pre-consolidation pressure ( $\sigma'_c$ ) which is the maximum overburden pressure that the soil sustained in the past, coefficient of consolidation ( $c_v$ ), which refers to the measure of the time it takes for a soil to consolidate, permeability ( $k$ ) or sometimes called hydraulic conductivity. Moreover, the stiffness moduli,  $M_0$  and  $M_L$ , are also evaluated from the stress versus strain diagram. Among these parameters that are obtained from this test, this master's thesis focuses on the effective stresses and the stiffness modulus, which play vital role in determination of the deformation properties of clay. The other parameters will be used as input data in different soil models in plaxis computer simulation.

#### **2.2.3.2 Triaxial test**

When the deformation analysis of soil is performed by an advanced soil model in Plaxis there is a need of a triaxial test. This because advanced models require more input of material data, for instance hardening soil model requires input of three modules, such as  $E_{oed}$  obtained from CRS test,  $E_{50}$  and  $E_{ur}$ , which are obtained by performing a triaxial test.

The triaxial test is a common test performed to determine the deformation properties, in this case compression modulus. In the test method a cylindrical soil sample is placed into the test equipment, which is filled with water, see Figure 12.

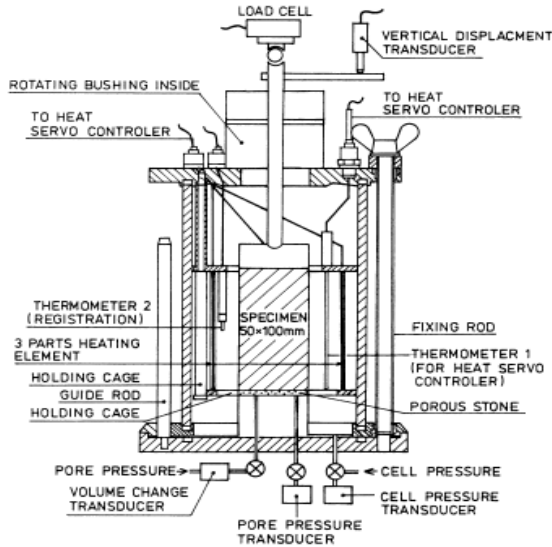


Figure 12: The triaxial test method equipment. (SGI, 1995)

By increasing the load on the sample an isotropic increasing stress can be obtained. The test is performed in two stages, which are consolidation and shearing. The following stress-strain relation can be obtained from the triaxial test, see Figure 13.

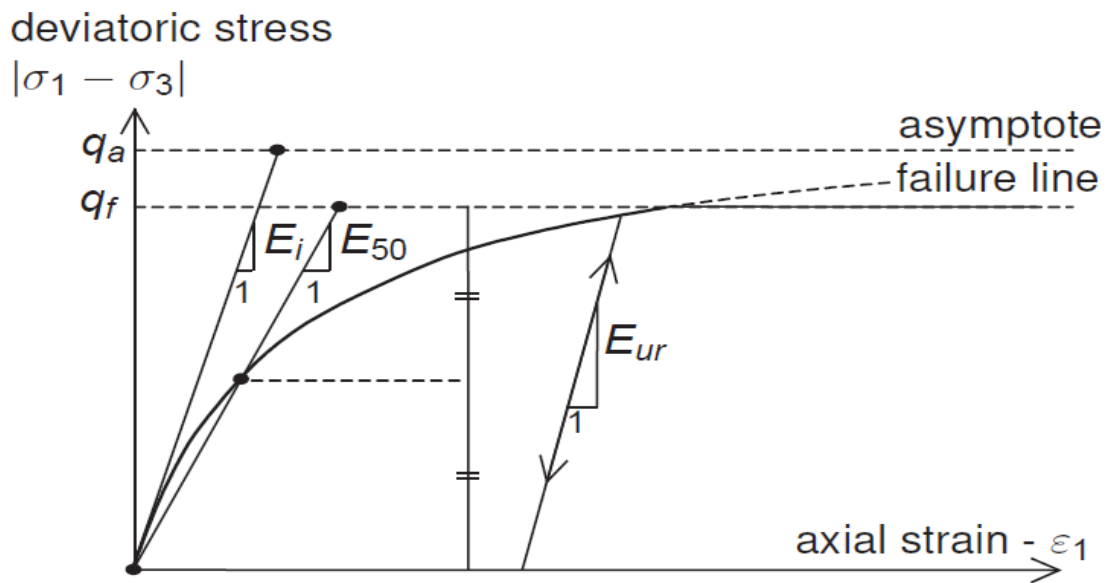


Figure 13: A standard drained triaxial test showing the hyperbolic stress-strain relation. (Brinkgreve et al, 2010)

As the figure shows unloading/reloading modulus,  $E_{ur}$  and secant modulus,  $E_{50}$  can be determined, which are important deformation parameters to be used as an input values in Plaxis deformation analysis.

### 2.2.3.3 Inclinometer

Horizontal deformations occur due to excavations, landslides, unstable slopes etc. A device called inclinometer is usually used to measure horizontal deformations due to these geotechnical problems. The instrument is installed before the construction begins, so that initial readings are collected. The device consists of a casing, a probe, a



control cable and a unit. Each component contributes some to perform measurement, see Figure 14. (Brouwer, 2007)



Figure 14: The inclinometer device. (Brouwer, 2007)

The casing, see Figure 15, is installed in a vertical borehole, which is situated in the soil layer where the deformations are expected. It is installed down to a depth where no deformations are expected to occur, and this is done so the casing will not rotate. It can also be installed in a way that it reaches the firm bottom (bedrock). (Brouwer, 2007)



Figure 15: The illustrations show a casing. (Brouwer, 2007)

When the ground moves, the casing anchored in the borehole will also move and by measuring the inclination and comparing to initial readings of the movement, the deformation is obtained. Usually the measurements are done twice by pulling up the inclinometer probe from bottom of the casing to top. The first measurement is done parallel to the inclinometer's wheel, which is the direction of the expected movement of the ground (A) and the second one is performed perpendicular to the wheel (B), see Figure 16. The movement of the ground is obtained by calculating the resultant of A and B axis. (Brouwer, 2007)

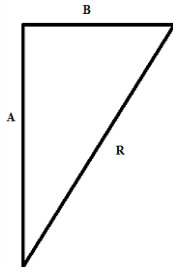


Figure 16: The movement of soil in two directions, A and B, and the resultant of the movements.

### 2.2.3.4 Gauges of timber

Another instrument used to measure deformations that occur due to slopes is the so called gauges. It is installed on the slope crests and is pressed down into the soil with a desired distance. The measurement points should be placed at the field in a way that they are near the profile and easy to make the readings. This surface deformation measuring instrument is installed with a desired number of points and in rows with a certain distance. The instrument measures the deformations in x-y-z directions.

## 2.3 Empirics

The different soil parameter values obtained both from field investigations and laboratory tests should be controlled. This is due to the fact that the parameter values from the tests have shown to be different from the one in real case. This value difference may arise due to change in conditions of the area due to different geotechnical works, or due to human and machine errors that occur while performing the field and laboratory tests. For this project, deformation due to excavation on clay, two important parameters, shear strength and stiffness modulus of clay are controlled with reasonable empirical relations.

### 2.3.1 Shear strength

The reduced shear strength evaluated from fall cone test and vane shear test can be controlled by a relation known as Hansbo's relation that uses pre-consolidation pressure and liquid limit, see equation (10).

$$\tau_{fu} = \sigma'_c * 0.45 * w_L \quad (10)$$

This empirical formula is applicable for soils that are normally consolidated and slightly over consolidated. The reduced shear strength of these types of soils obtained from the fall cone test and vane shear test can then easily be controlled by using the above relation. If the reduced shear strength values obtained from the tests are high, then one can conclude that a higher correction factor is used. But, if it is the reverse case, further investigations shall be carried out in order to obtain a reasonable shear strength value. (Larsson, 2008)

### 2.3.2 Modulus

The stiffness modulus,  $M_0$  obtained from the CRS-test should be controlled, since the value obtained from the test can be different from the actual value in field. Especially the unloading modulus, the modulus of soil where there is considerable excavation, is expected to have a higher value than the one obtained from the CRS test, since the shear strain around the excavation area is expected to be small. To estimate a reasonable value of the unloading modulus, different empirical approaches are proposed by different persons. These empirical approaches use different soil parameters from the lab and field tests.

The first approach uses pre-consolidation pressure as a parameter for the empirics see equation (11). This is the equation used in the tender document for the actual case to perform the deformations analysis.

$$M_0 = 50 * \sigma'_c \quad (11)$$

The second approach used in this thesis to obtain the compression modulus, uses the undrained shear strength as a parameter, see equation (12). This empiric approach is only used in hardening soil model.

$$M_0 = 250 * C_{uk} \quad (12)$$

The other empirical relation uses a factor to increase the oedometer modulus;  $M_0$ , where it is not possible to perform unloading and reloading test to determine the real modulus, see equation (13) (Sällfors 2001).

$$M_0 = (3 \text{ to } 5) * M_{0,CRS} \quad (13)$$

Another empirical approach to estimate the unloading modulus of clay is proposed by Jenny Persson, based on field tests from the construction site at Lilla Bommen. In this approach, the unloading modulus is estimated by taking the maximum of two formulas that have change in value of OCR range of 1.5 to 2 see equation (14).

$$M_{ul} = \max \left\{ \begin{array}{l} \sigma'_c * A * \left( \frac{1}{OCR} \right)^4 \\ \frac{\sigma'_c}{OCR/as} \end{array} \right. \quad (\text{Persson, 2004}) \quad (14)$$

Where the values,  $A = 1500$  and  $as$  is in the range of 0.0025 to 0.005.

The last approach to determine the unloading secant modulus is using the outcome from FE-analysis performed with the MIT-S1 soil model. The parameter set has been studied in detail by Kullingsjö (2007). The MIT formulation is based on field tests and laboratory tests, which shows how the unloading modulus varies with change of OCR and vertical over consolidation pressure. It is presented in the form of chart, and it also consists of different approaches proposed by different researchers. It is shown in Figure 17 below. This approach and the second approach see equation (12), give similar unloading modulus as the one stated in the tender document, see equation (11). Due to this the unloading modulus from the tender document and the second approach are used in Plaxis simulation, since the deformations results for all three moduli are expected to be similar.

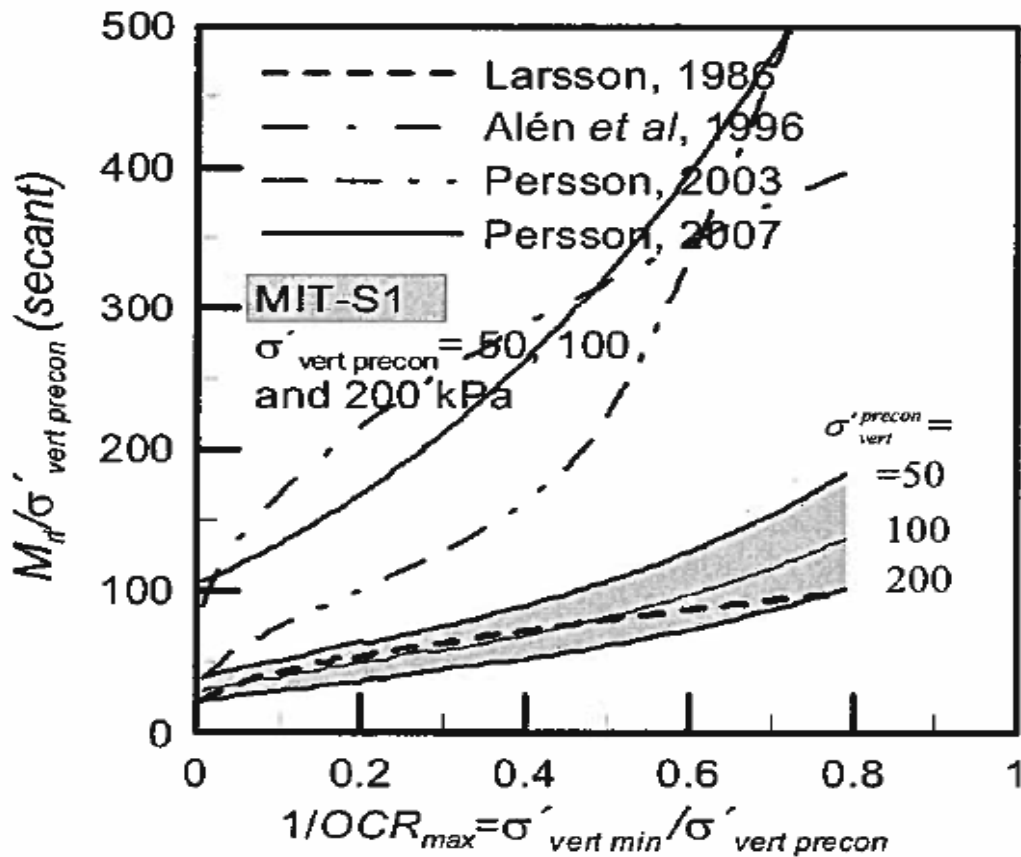


Figure 17: Comparison of different approaches for unloading modulus (Kullingsjö, 2007)

## 2.4 Plaxis

In different geotechnical applications, Plaxis, a two dimensional finite element based computer program, is used for simulation purpose. This sophisticated computer program is mainly used for analysis of deformation and stability. It has advantageous feature that enables users to choose different soil models, which is dependent on mechanical deformation behaviours of soil, for the simulation. In this project, among the different soil models, Mohr coulomb (MC) and hardening soil (HS) models are chosen for the deformation analysis. The basic principles and assumptions in these models are discussed in detail later.

### 2.4.1 Input

The purpose of the input program is to create the geotechnical finite element model, to define and assign material properties and to generate the initial stress with in the soil layers and boundary condition. To create the geometry of the model, points, lines, and clusters (areas) are used. Different types of geotechnical and structural elements can be inserted into the model. The fixity and support system of the elements are also defined depending on the conditions of the application. Additionally, different types of loads and boundary conditions can be defined. The material properties definition stage involve inserting different soil parameters like young's modulus (E), cohesion(c), poisons ratio ( $\nu$ ), friction angle ( $\phi$ ), and dilatancy angle ( $\Psi$ ) into the

program. These soil parameters can be different for different soil models. The method of analysis, drained or undrained, is also defined here. Once all these are performed, a mesh in form of small triangles connected to each other can be generated. The finer the mesh is, the complexity of analysis of the model increases, but the accuracy, on the other hand also increases. The phreatic level that shows the level and orientation of the ground water is another important aspect to be defined in the input program. Before proceeding to the calculation part, initial stress level of the soil is generated by using the Ko- procedure or the gravity loading. (Brinkgreve et al, 2010)

## **2.4.2 Calculation**

The calculation program is the part of the whole simulation where the analysis of the created model is performed. The procedure is started by defining the initial stage or the already created finite element model in the input program. Then the other construction stages can be defined, otherwise the program only simulates the model defined from the input program. Plaxis offers three types of calculation modes for the users. These include, plastic, where the deformation is expected to be elastic-plastic, consolidation, where the development of or dissipation of excess pore pressure in the clay is considered, and phi-c reduction, a safety analysis by reducing the strength parameters of the soil. In this calculation part there are also load stepping and control, and load incremental multipliers option where the user can insert appropriate value depending on the conditions of the application. Additionally, sensitivity analysis can be performed to determine the influence of individual parameters on the output of the simulation. Before the final calculation is started, specific points can be selected to generate load-displacement curves and stress path or stress strain curves for those points. (Bringreve et al, 2010)

## **2.4.3 Output**

In Plaxis, the results from the overall simulation can be obtained from the output program. It mainly emphasizes on results of generated input data and finite element based calculation. The outputs can be in the form of plots of full model, or plots of special objects of the model and in the form of tables. For a specific output, the result can be presented in the form of arrows, contours and shadings. Different types of outputs can be obtained from the simulation, choosing the important results will depend on the purpose of the simulation and the choice professional performing the simulation. The outputs obtained from Plaxis include, deformed mesh of the whole model, different types of deformations and strains and effective and total stresses. For structural and geotechnical elements, the possible outputs from the simulation consist of deformations, axial shear forces and bending moments. For a particular section, where results from that section are relevant, Plaxis offers a way to view the outputs in that section inform of cross-section. Load-displacement curves and time-displacement curves can also be generated for those specific points which were selected before running the calculation. All the relevant outputs from the simulation can be documented in report form. (Bringreve et al, 2010)

## 2.4.4 Soil models

In Plaxis, different soil models are available in order to carry out appropriate simulation for different types of geotechnical applications. These models include the Mohr coulomb (MC), joint rock (JR), hardening soil (HS), soft soil (SS), and modified cam-clay model. As mentioned earlier, among the listed soil models, for this project, Mohr coulomb (MC) and hardening soil (HS) are chosen to be used. This is due to these models are assumed have features that take into consideration the characteristics and aim of this project.

### 2.4.4.1 Mohr coulomb (MC)

The main concept behind the Mohr coulomb method of analysis is that failure in soils occurs when the applied shear stress is equal to the shear strength of the soil. As shown in figure (18), the Mohr circle is drawn on Cartesian coordinate of principal stress versus shear stress. Failure in the soil occurs when the Mohr circle touches the failure envelope line. By performing laboratory tests under undrained conditions the shear stress,  $\tau_f$  is equal to the undrained shear strength,  $c_{uk}$  at failure. It can be explained with equation (15).

$$\tau_f = c = (\sigma_1 - \sigma_3)/2 \quad (15)$$

$\sigma_1$  - Major principal stress in the vertical direction

$\sigma_3$  - Minor principal stress in the horizontal direction

The cohesion  $c'$  and the friction angle  $\phi'$  can be determined from the failure envelope line from laboratory tests performed under drained conditions. The shear strength will be a function of the cohesion  $c'$  and the friction angle  $\phi'$  see equation (16).

$$\tau_f = c' + \sigma_f \tan \phi' \quad (16)$$

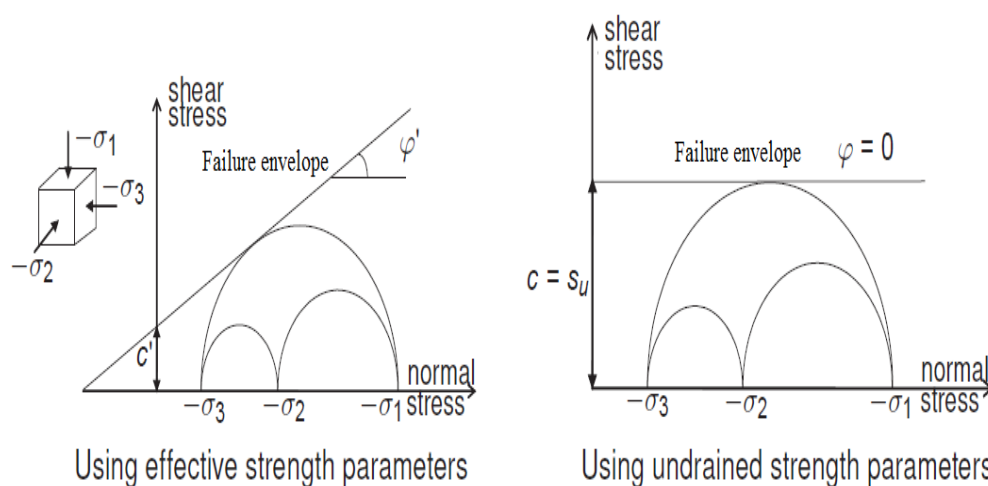


Figure 18: Mohr coulomb failure criterion with effective and undrained strength parameters. (Bringreave et al, 2010)

Mohr coulomb is a linear elastic perfectly plastic model, which means that this model describes material behavior as elastic within a certain defined area and outside of it plastic, sees Figure 19.

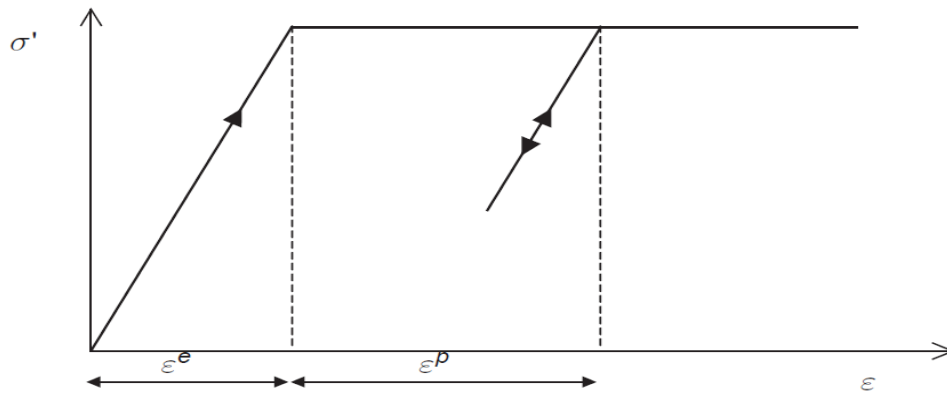


Figure 19: The figure shows the main idea of an elastic perfectly plastic soil model. (Bringreve et al, 2010)

The calculations in a Plaxis simulation by using Mohr coulomb model are fast and therefore the model is usually used to obtain a first view of the problem. Five different parameters are required to perform a simulation in Plaxis software by using Mohr coulomb. The parameters required are the following; Young`s modulus E, poison`s ratio  $\nu$ , friction angle  $\phi$ , cohesion c and angle of dilantancy  $\psi$ . The selected modulus of elasticity, E is an average value of the modulus, which increases linearly with depth by an increment  $E_{\text{increment}}$ . The modulus of elasticity (Young`s modulus) is obtained from a triaxial test or a CRS-test. If the modulus is obtained by use of a CRS-test, the modulus,  $E_{\text{eod}}$  has to be transformed to an elasticity modulus, E by the equation (17).

$$E_{\text{oed}} = \frac{(1 - \nu) * E}{(1 - 2 * \nu) * (1 + \nu)} \quad (17)$$

If effective values of elasticity modulus, E and poison`s ratio,  $\nu$  are used in Plaxis software to perform a simulation, the equation (18) has to be used to transform the elasticity modulus into an effective one. (Bringreve et al, 2010)

$$E' = \frac{2 * (1 + \nu') * E}{3} \quad (18)$$

#### 2.4.4.2 Hardening soil model (HS)

Hardening soil model is an advanced soil model which is used to analyze the non-linear behavior of soil by taking into account a change of the stiffness modulus by a change of the soil stresses due to compression and/or shearing of the soil. This feature makes this model to be different from Mohr coulomb model which assumes the soil to have elastic-perfectly plastic behavior. The hardening soil model also allows a more precise soil modeling by taking into consideration the pre-consolidation pressure. In Plaxis this can be performed by use of OCR (Over Consolidation Ratio) and POP (Pre Overburden Pressure), see Figure 20.

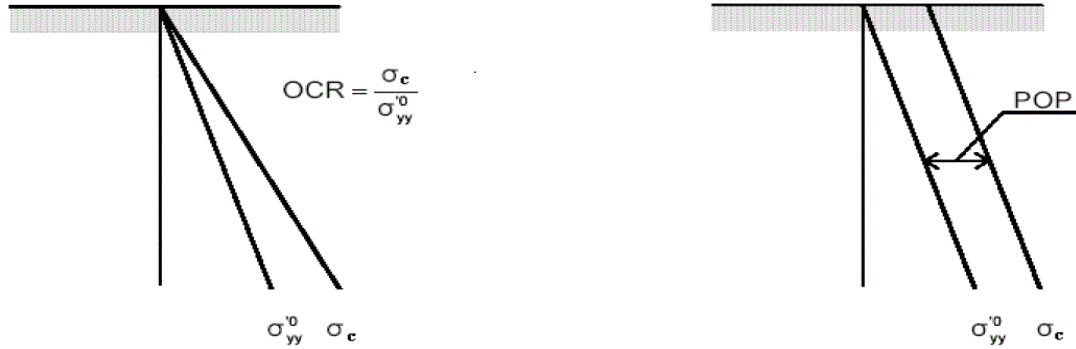


Figure 20: The definition of over consolidation ratio by OCR and POP. (Bringreve et al, 2010)

The insertion of the pre-consolidation pressure into the model is based on the fact that for stresses higher than the pre-consolidation pressure the stress strain curve gives a modulus,  $M_L$  that is smaller than the elastic modulus  $M_0$ , see Figure 21.

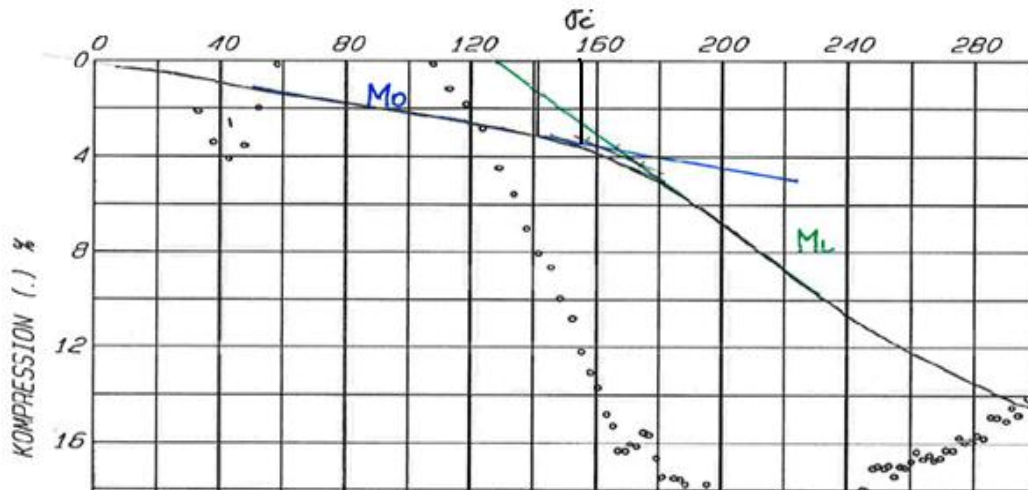


Figure 21: Stiffness modulus at elastic ( $M_0$ ) and plastic ( $M_L$ ) region obtained from CRS test.

The modulus in the hardening soil model is described more accurately by adding three moduli;  $E_{ur}$ , which refers to reloading/unloading modulus and  $E_{50}$  and  $E_{oed}$ .  $E_{50}$  refers to secant modulus from tri-axial test and  $E_{oed}$  refers to tangent modulus that corresponds to a modulus for stresses higher than the pre-consolidation pressure evaluated from the CRS test, see figure above. (Bringreve et al, 2010)

These moduli are stress dependent and in the following formulas the change of the three moduli can be observed by the change of soil stress (by the depth), see the equations (19), (20), & (21) below. (Bringreve et al, 2010)

$$E_{50} = E_{50}^{ref} \left( \frac{c \cos \phi - \sigma'_3 \sin \phi}{c \cos \phi + p^{ref} \sin \phi} \right)^m \quad (19)$$

$$E_{oed} = E_{oed}^{ref} \left( \frac{c \cos \phi - \sigma'_1 \sin \phi}{c \cos \phi + p^{ref} \sin \phi} \right)^m \quad (20)$$



$$E_{ur} = E_{ur}^{ref} \left( \frac{c \cos\phi - \sigma'_3 \sin\phi}{c \cos\phi + p^{ref} \sin\phi} \right)^m \quad (21)$$

In the above mentioned formulas the  $E^{ref}$  is the reference Young's modulus and  $p^{ref}$  is reference stress for the stiffness and is set to 100 kPa, as a default value in Plaxis. Usually  $E_{ur}^{ref}$  is set to three times  $E_{50}^{ref}$  and  $E_{cod}^{ref}$  is set to be equal to  $E_{50}^{ref}$  as a default value of the Plaxis software. However Plaxis cannot handle to big ratios between  $E_{50}^{ref}$  and  $E_{cod}^{ref}$  and therefore Plaxis software will sometimes recommend a value of one of the modulus to use. The exponent,  $m$ , is a factor that regulates the stress-dependence of the modulus. For soft soils the factor is set to 1 and for sands it is set to value from 0.5 to 1. In the formulas it can also be noticed that  $E_{cod}$  is dependent of the major principal stress  $\sigma_1$ ,  $E_{ur}$  and  $E_{50}$  are dependent on the minor principal stress  $\sigma_3$ . The following formula is used to determine the horizontal stress, see equation (22). (Bringreave et al, 2010)

$$\sigma_3 = K_0 * \sigma_1 \quad (22)$$

Figure 22 shows the vertical and horizontal stresses varying with depth and also which depth  $P^{ref} = 100$  kPa corresponds to.

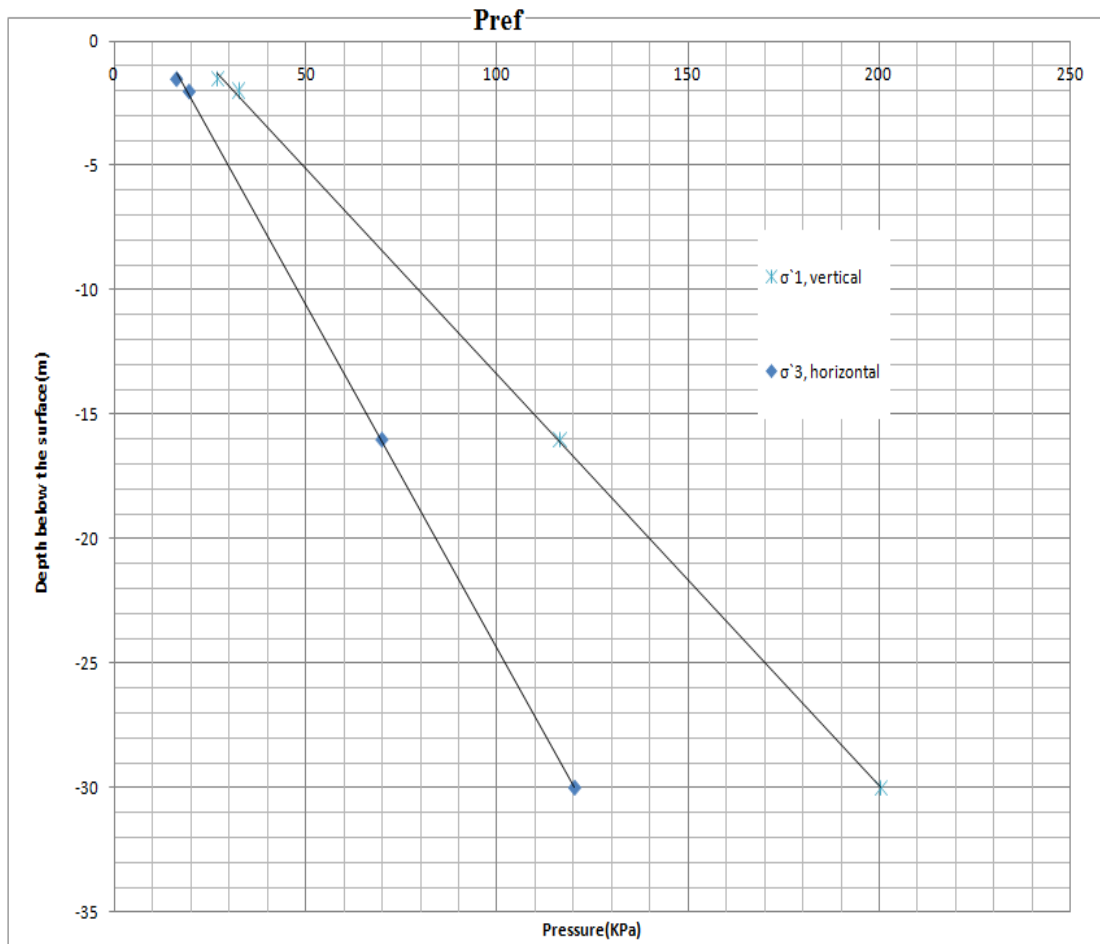


Figure 22: Effective vertical, horizontal stresses and reference stress.

Poisson's ratio for unloading/reloading and the soil pressure coefficient,  $K_0$  are other parameters needed to describe the deformation properties of a soil by use of hardening soil model.

The failure parameters in this model are the same as the parameters for failure in Mohr coulomb soil model. These include friction angle,  $\phi$ , cohesion,  $c$ , and angle of dilantancy,  $\psi$ . Due to this a safety analysis in hardening soil model will give the same safety factor as the one obtained from Mohr Coulomb soil model. (Brinkgreve et al, 2010)

### 3. Deformations analysis of section E13

In this chapter, area description, soil profile and properties of different soil parameters that are relevant to this thesis are presented. The excavation procedure is also described in this chapter and in the end the deformation measurement is presented.

#### 3.1 Area description

The bridge, where the excavation is taking place, is located in the stretch km 471+600 – 472+100, see drawing below. It is decided to use the field and laboratory data from boreholes 71003, FB41, 71007 and SYD. These boreholes were selected, because of their close proximity to the section and because they are located in the actual stretch, in which the bridge and the excavation are supposed to be designed and performed for. This is shown in Figure 23.

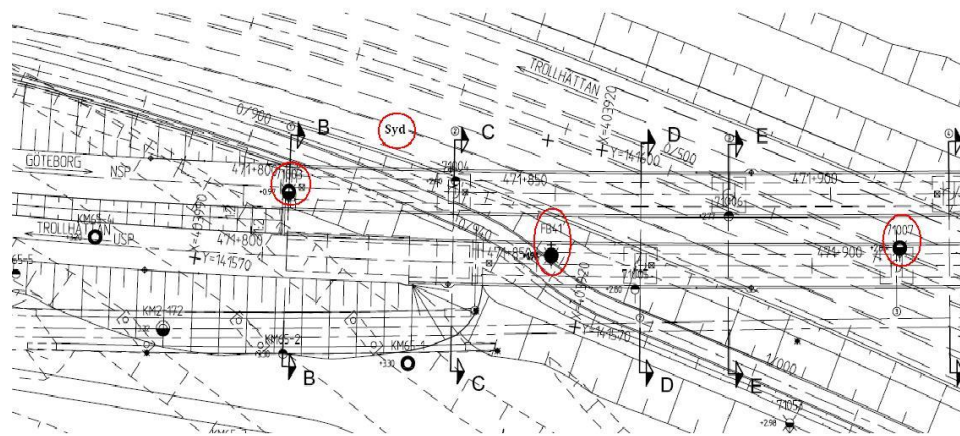


Figure 23: The red circles shows the selected boreholes, 71003, FB41, 71007 and Syd.

#### 3.2 Topography

The area, where the excavation is taking place is located on the east side of Göta River. The area is characterised by its low-lying landscape. The level of the ground in the specific stretch varies from +1 meter to +3 meters above sea level.

#### 3.3 Pore water pressure

The pore water pressure investigation has been performed 4-6 times at different seasons of the year in order to take into account the pore pressure seasonal variation. The result obtained from the pore water measurements in the stretch km 471+600 – 472+100 shows that the level of the groundwater begins at level +1.5, which means 1.5 meters below the ground surface. The results obtained also show that the pore pressure is hydrostatic from level +1.5, where the groundwater begins, to level -3. From the level -3, which is 6 meters below the ground surface the pore pressure increases with 10.5 kPa/m.

### 3.4 Soil profile

The soil profile is obtained from cone penetration and pressure probing tests performed in the field. In the stretch km 471+600 – 472+100, the first 2 meters of the soil consists of silty sand, which begins at level +3 and finishes at level +1. Below the silty sand layer there is a deep layer of soft clay, which is approximately 36 meters deep. The soft clay layer begins at level +1 and finishes at level -35. Beneath the soft clay, there is a massive layer of frictional material, see Figure 24.

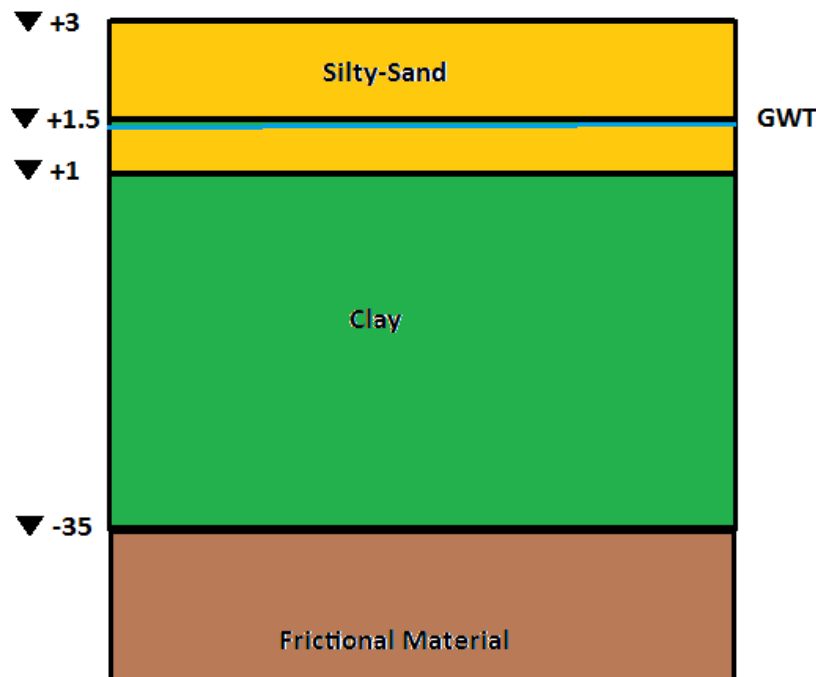


Figure 24: Soil profile for the area.

### 3.5 Soil parameters

In this project, the important soil parameters that are evaluated from field and laboratory tests are studied in order to determine the deformation properties of the soil in the stretch km 471+600 – 472+100, where the excavation under the bridges is taking place. Moreover, careful attention is given during the evaluation process, since, the soil parameter values will be used as an input in Plaxis computer deformation analysis. The important soil parameters studied in this thesis are discussed below and are presented in the form of parameter versus depth. Note that the surface level in the actual section begins at +3 and it is represented as depth  $\pm 0$  m in all the diagrams and this way of representation continues throughout the depth.

#### 3.5.1 Density

The density is obtained by evaluating the laboratory data from two boreholes within the actual stretch. The density is between 1.5-1.7 t/m<sup>3</sup> through the entire clay layer, see Figure 25.

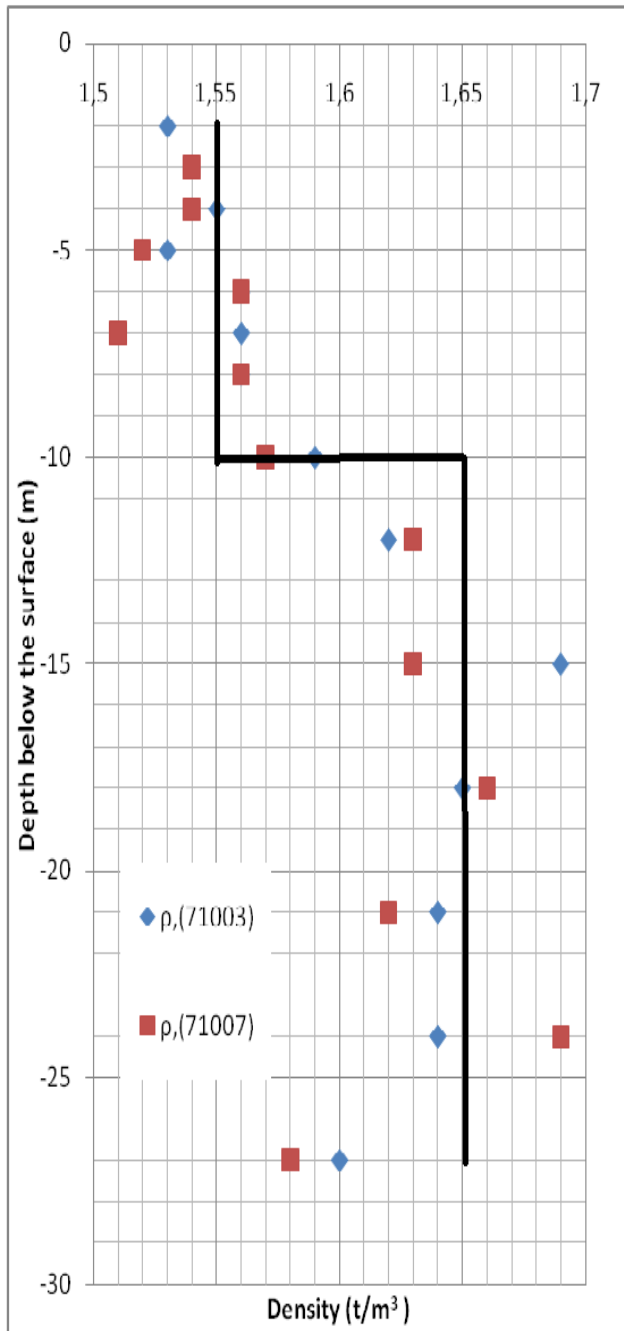


Figure 25: The density of the clay in the area.

### 3.5.2 Water content

The water content of the clay layer is 60-90 % and is obtained from two boreholes, see Figure 26.

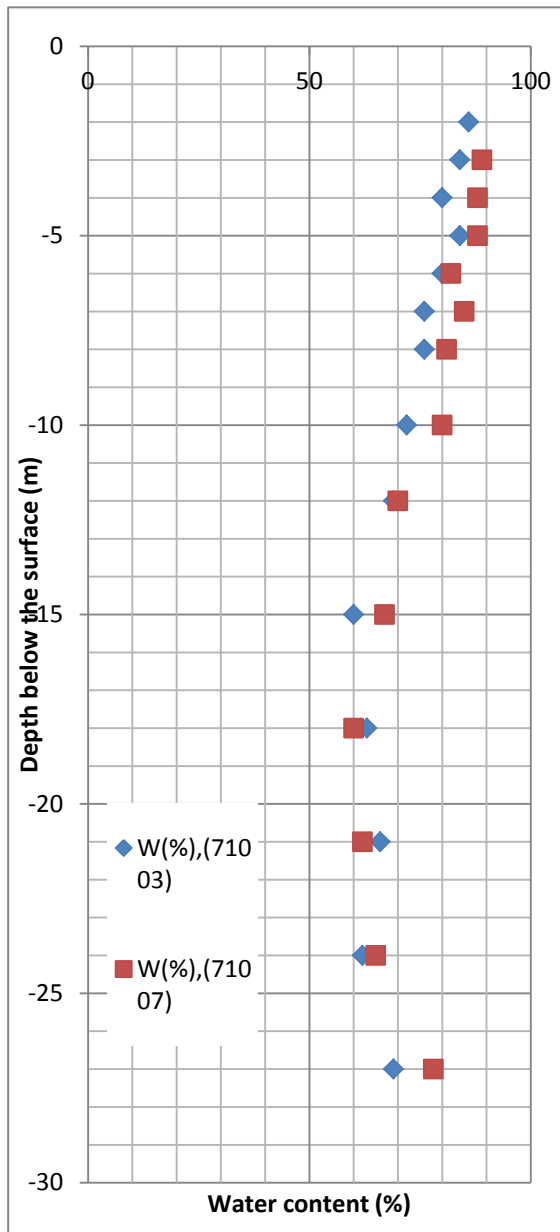


Figure 26: The water content of the clay in the area.

### 3.5.3 Liquid limit

The liquid limit is between 60-80 %, see Figure 27.

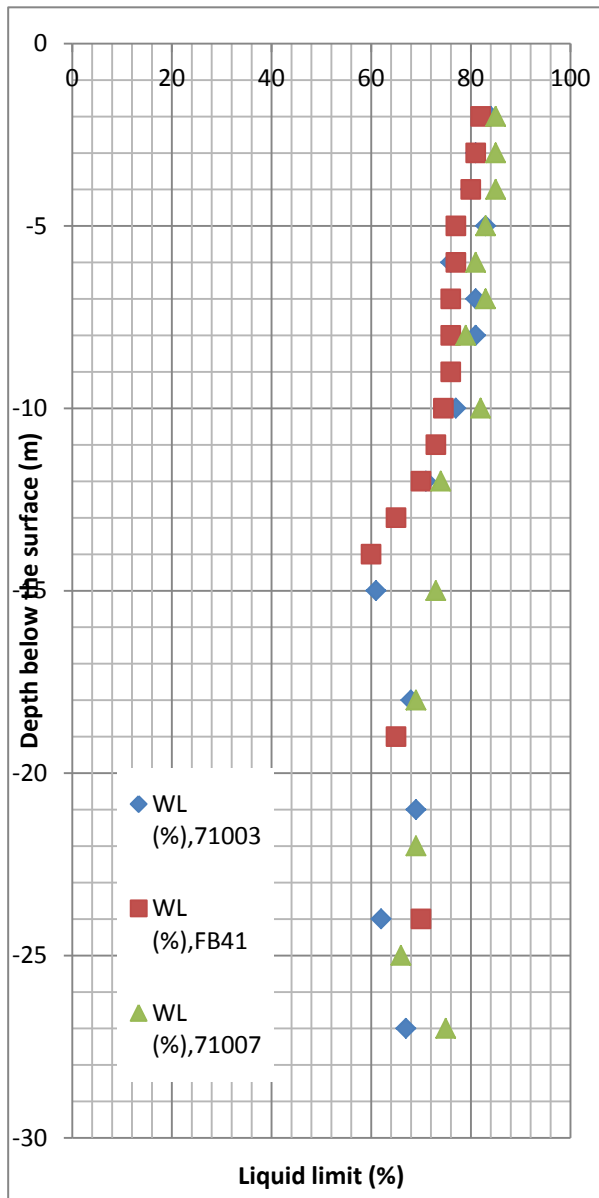


Figure 27: The liquid limit of the clay in the area.

### 3.5.4 Sensitivity

The sensitivity of the clay has a value in range of 15 to 30. This shows that the clay is sensitive, but not that much sensitive when compared with quick clay where the sensitivity is over 50, see Figure 28.

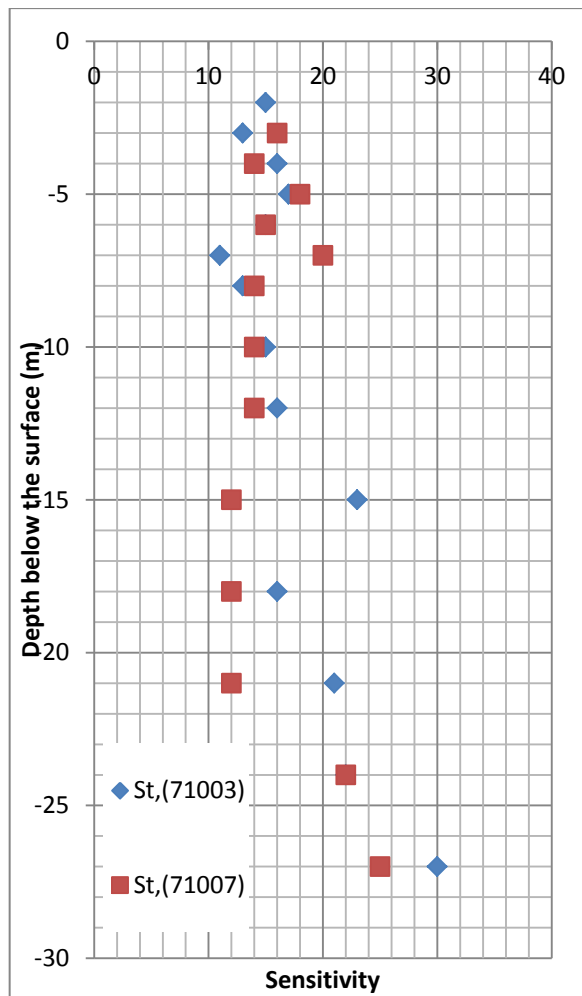


Figure 28: The sensitivity of the clay.

### 3.5.5 Shear strength

The data for the shear strength from the selected boreholes were collected from different kinds of tests; fall cone test and vane shear test.

For results from vane shear test and fall cone test, a correction factor,  $\mu$ , has been used to reduce the unreduced shear strength,  $\tau$ , from the different tests. The reduced shear strengths from the selected boreholes were plotted in the diagram, see figure 29 shown below and two equations describing the reduced shear strength along the clay layer 1 and clay layer 2 is generated.



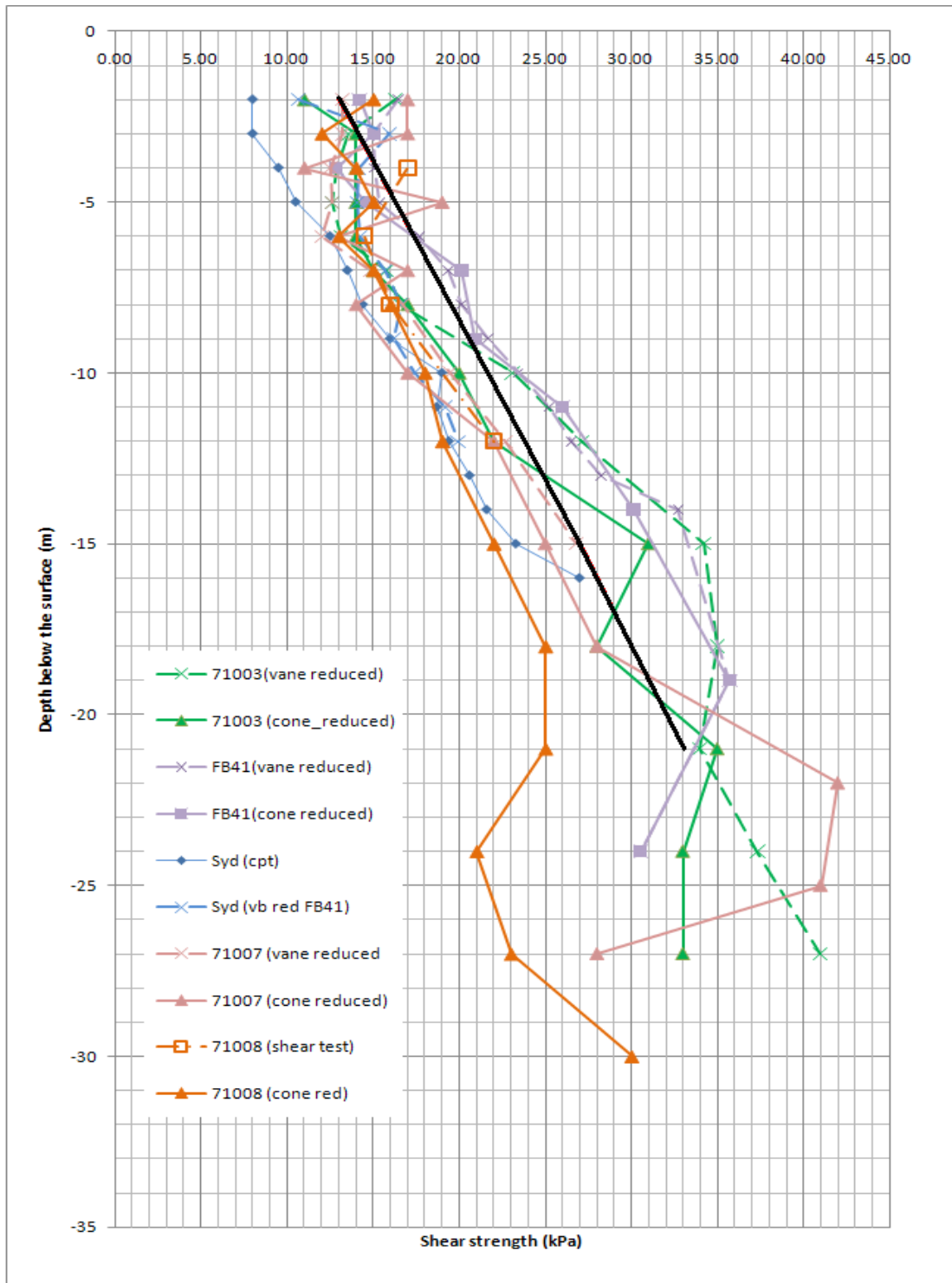


Figure 29: Shear strength evaluated from different boreholes in the actual stretch.

The final trend line of all the shear strength evaluated from the different boreholes shows, the clay layer has approximated shear strength value of 15 kPa in the beginning which is constant for more or less 7m below and increases afterwards with depth. However, to follow the increase of stiffness in the soil and to make the Plaxis simulation less complicated, the clay layer is divided into two layers with shear strength profile that corresponds with the above figure. The generated equations for the shear strength, which is represented by the black line in the shear strength figure in the two clay layers are as follows;  $Cu1 = 13 + 1/m$  kPa  $Cu2 = 27 + 1/m$  kPa

The formula shows that the shear strength is 13 kPa in the beginning of the first clay layer and increases with 1 kPa each meter up to a depth of 13 meters where the second clay layer begins. The second clay layer has initial shear strength of 27 kPa and increases with 1 kPa each meter to the end of the clay layer. The equations describing the shear strength properties of the clay profile are compared with the empirical values according to Hansbo's relation. The comparison shows that the reduced shear strength values obtained from the tests are low, and therefore further investigations shall be carried out in order to obtain a reasonable shear strength value.

### 3.5.6 Effective stresses and pre-consolidation pressure

Over consolidation ratio, OCR is determined by comparing the pre-consolidation pressure with the effective stresses of the ground. The OCR varies between 1.1-1.3 from the beginning of the clay layer to the end, which means that the clay is slightly over-consolidated, see Figure 30. The pre-consolidation pressure is evaluated from CRS-test for three boreholes within the actual stretch.

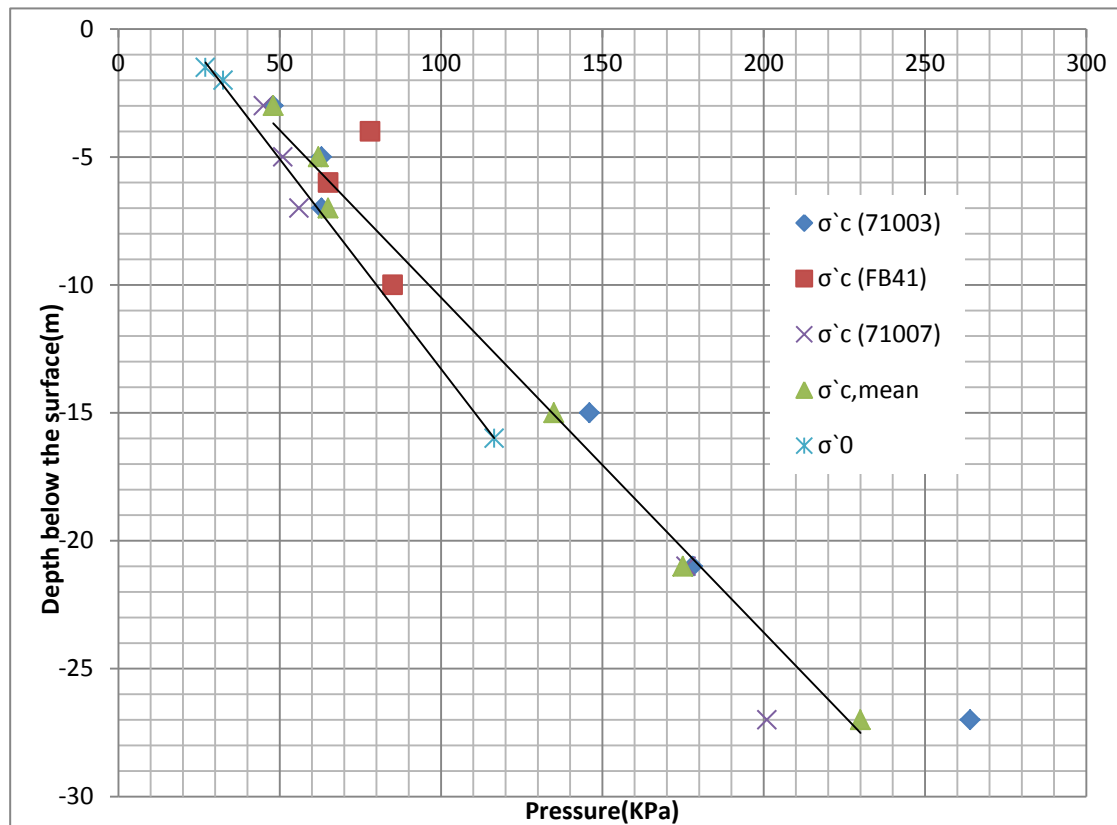


Figure 30: The diagram shows the insitu effective stresses and preconsolidation pressures evaluated from CRS-test.

### 3.5.7 Permeability

The permeability is evaluated from three boreholes within the actual stretch. The permeability of the clay layer is between  $0.5 \cdot 10^{-9}$  -  $9 \cdot 2 \cdot 10^{-9}$  m/s, see Figure 31.

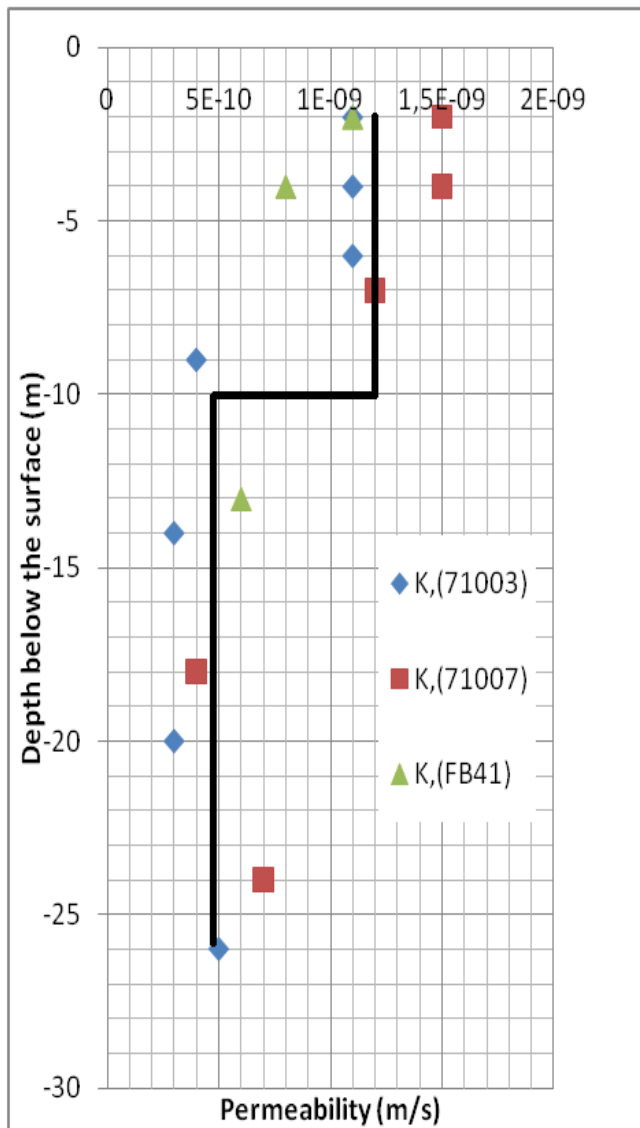


Figure 31: The permeability of the clay in the area.

### 3.5.8 Stiffness modulus

The compression modulus determined from oedometer test and also from the different approaches in earlier section is presented here, see Figure 32.

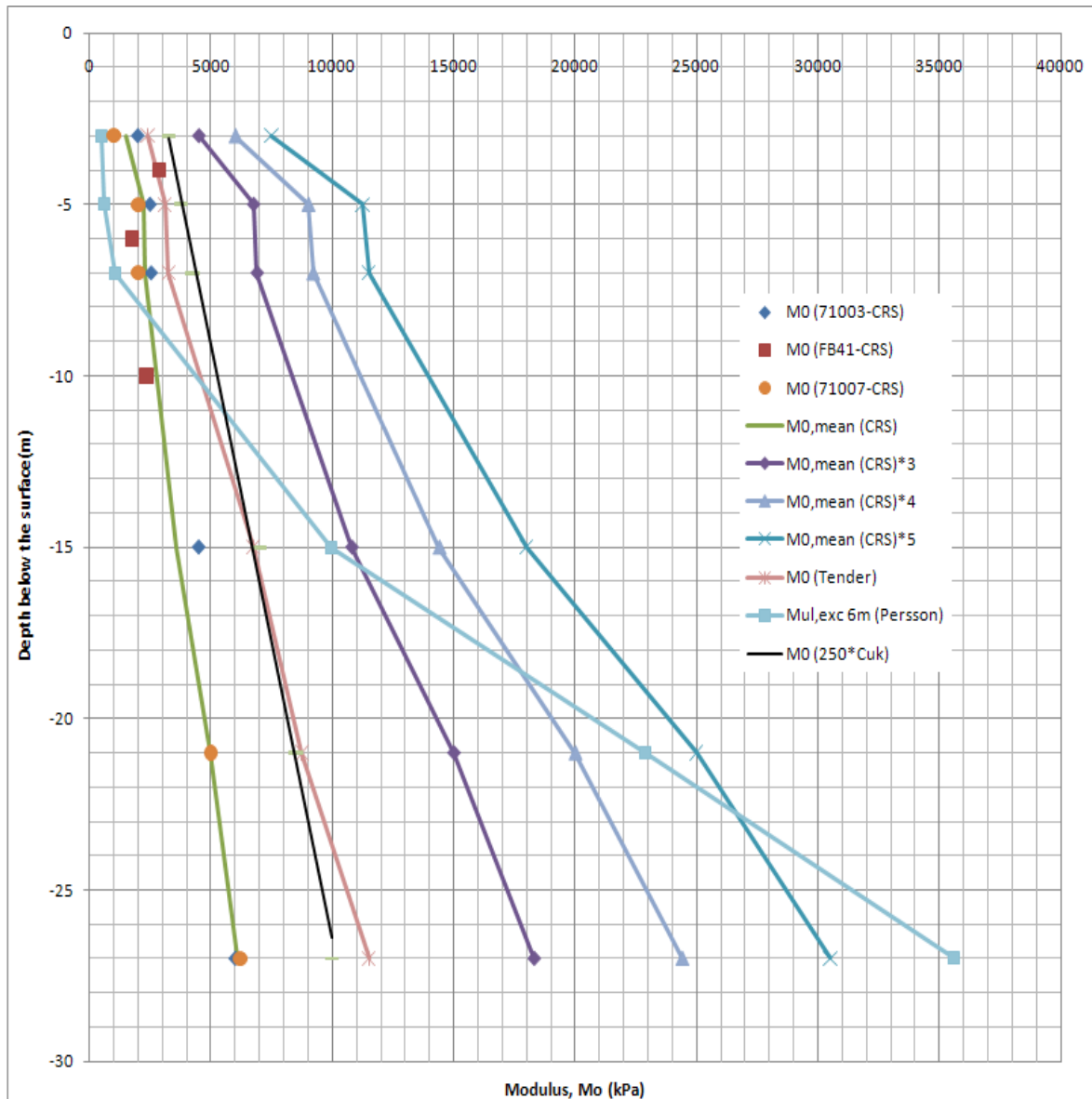


Figure 32: Stiffness modulus from oedometer test and different empirical approaches.

### 3.6 Excavation procedure

The excavation in section E13 is carried out by slope stability measures. If the excavation is done with too steep slopes, ground failure will occur. Ground failure occurs when the mobilized shear stress is higher than the available shear strength of the ground, i.e.  $F < 1$ , see equation (23) below.

$$F = \frac{\tau_f}{\tau_m} \quad (23)$$

The excavation in section E13 was performed to a depth of 6 meters below the ground surface with a width of 30 meters. The excavation in this project is done in two stages. The first one is 2 meters below the surface and the second is 4 meters below the first excavation stage, see Figure 33.

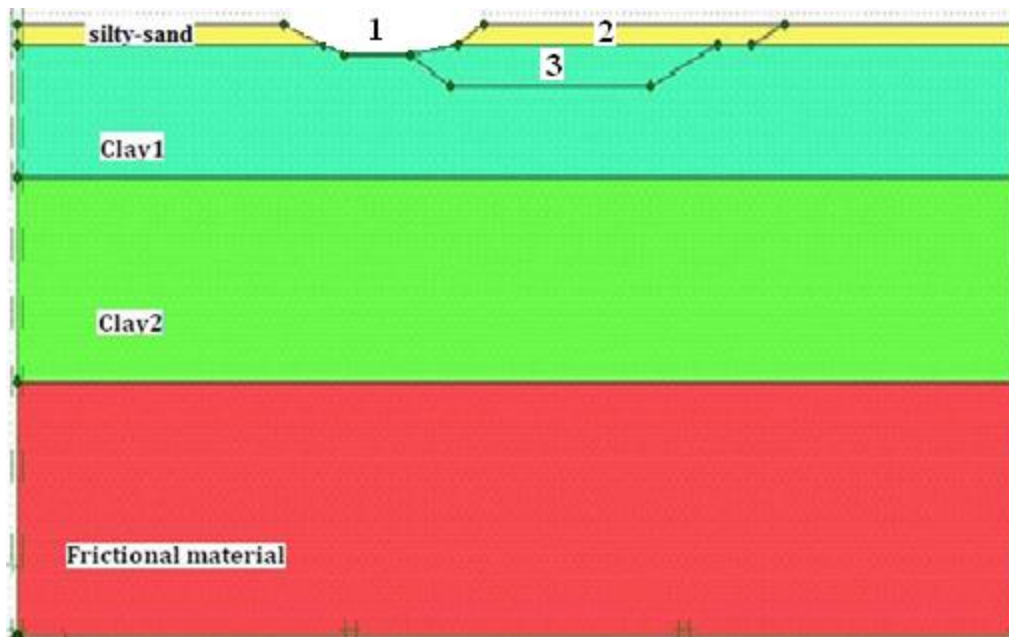


Figure 33: Excavation stages: stage 1, excavation of old E45, which was excavated 50 years ago, stage 2 &3, excavation under the railway bridge for the new E45.

The excavation is performed in a way that the slopes will have a safety factor around 1.4, which means that no ground failure will occur, see Figure 34.

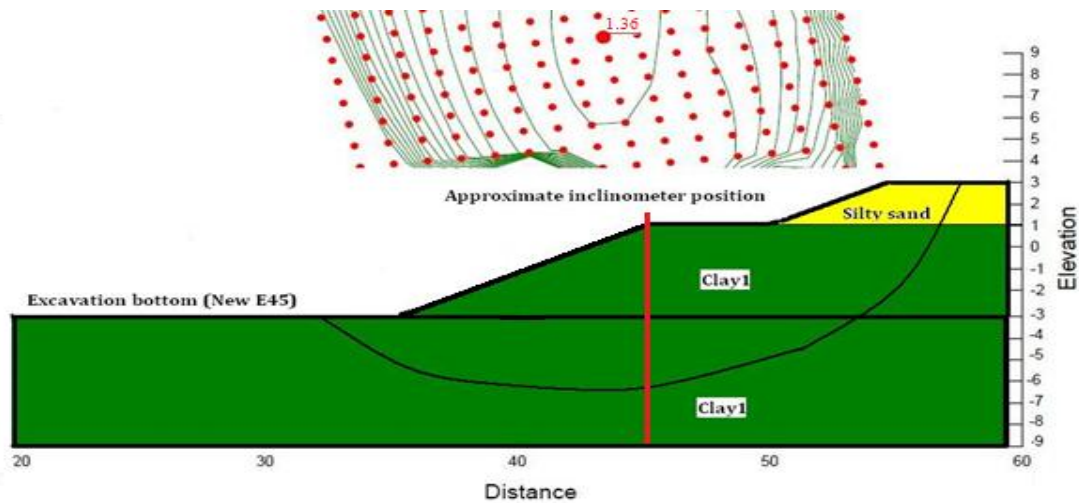


Figure 34: Slope stability.

### 3.7 Deformation measurement

The horizontal deformations in section E13 is measured by inclinometer and gauges of tree at different points at the actual stretch.

A measurement program is installed on the eastern slope crest with two rows of data points. The measurement points consist of gauges of timber, which are pressed down at least one meter below the surface of the ground. The first line is installed about two meters from the slope crest and the second line is installed about 15 meters from the slope crest. The distance between the points is about 20 meters from the slope crest.



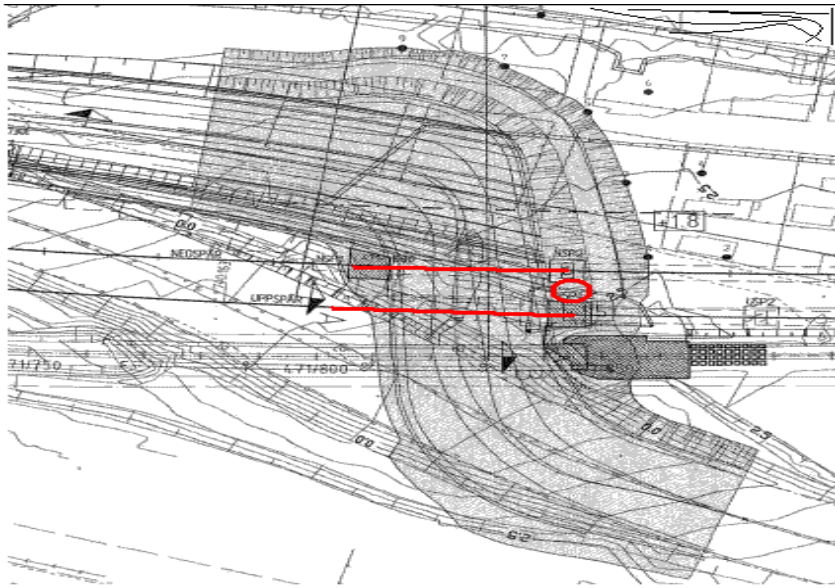


Figure 37: Position of the inclinometer between the two bridges.

### 3.7.1 Inclinometer readings

The measured cumulative resultant horizontal displacements in the current section in inclinometer position can be seen in Figure 38.

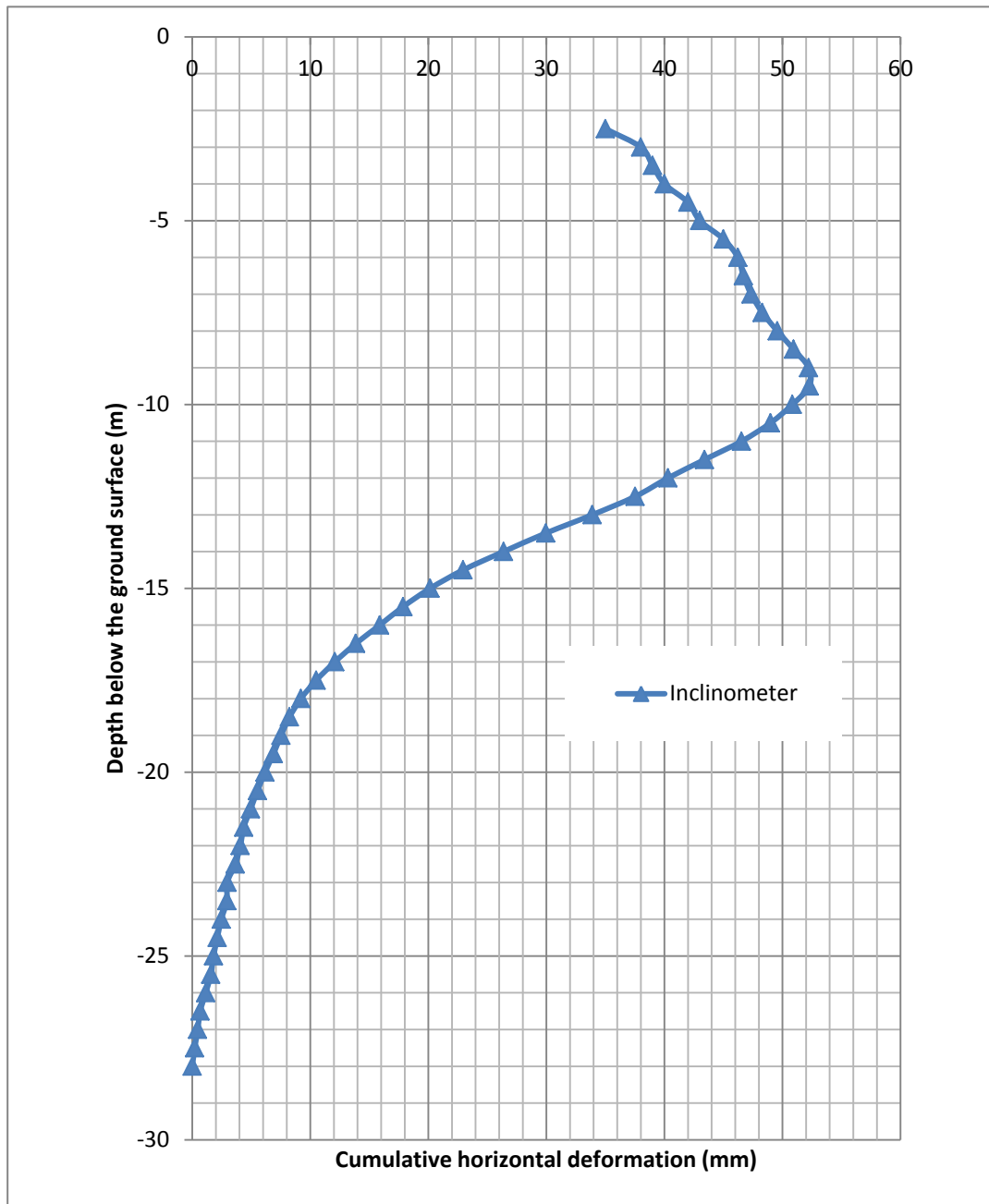


Figure 38: Cumulative resultant horizontal deformations by inclinometer device.

The above presented diagram shows that there is no horizontal movement below a depth of 27 meters down. As it can be seen the maximum horizontal deformation is occurring around a depth of 9 meters below the ground surface. The horizontal movement curve is showing that the deformation is decreasing from the depth of 9 meters to the upper level of the clay. This decrease in value is due to the situation around the bridge foundation, which is discussed more in Outputs chapter.

### 3.7.2 Gauges readings

As mentioned in section 3.7, a study of the horizontal movement at the surface of the slope crest has been performed. The measurement consists of points that measure the movement in x, y and z directions.



Only in points 7, 8 and 9 the cumulative horizontal deformation has been analysed because of their close distance to the studied section in Plaxis. In Figure 39 the horizontal deformations are presented with time. The dates of interest are between November 29<sup>th</sup> 2010 and February 7<sup>th</sup> 2011, because the excavation stages for the new E45 are performed between these dates.

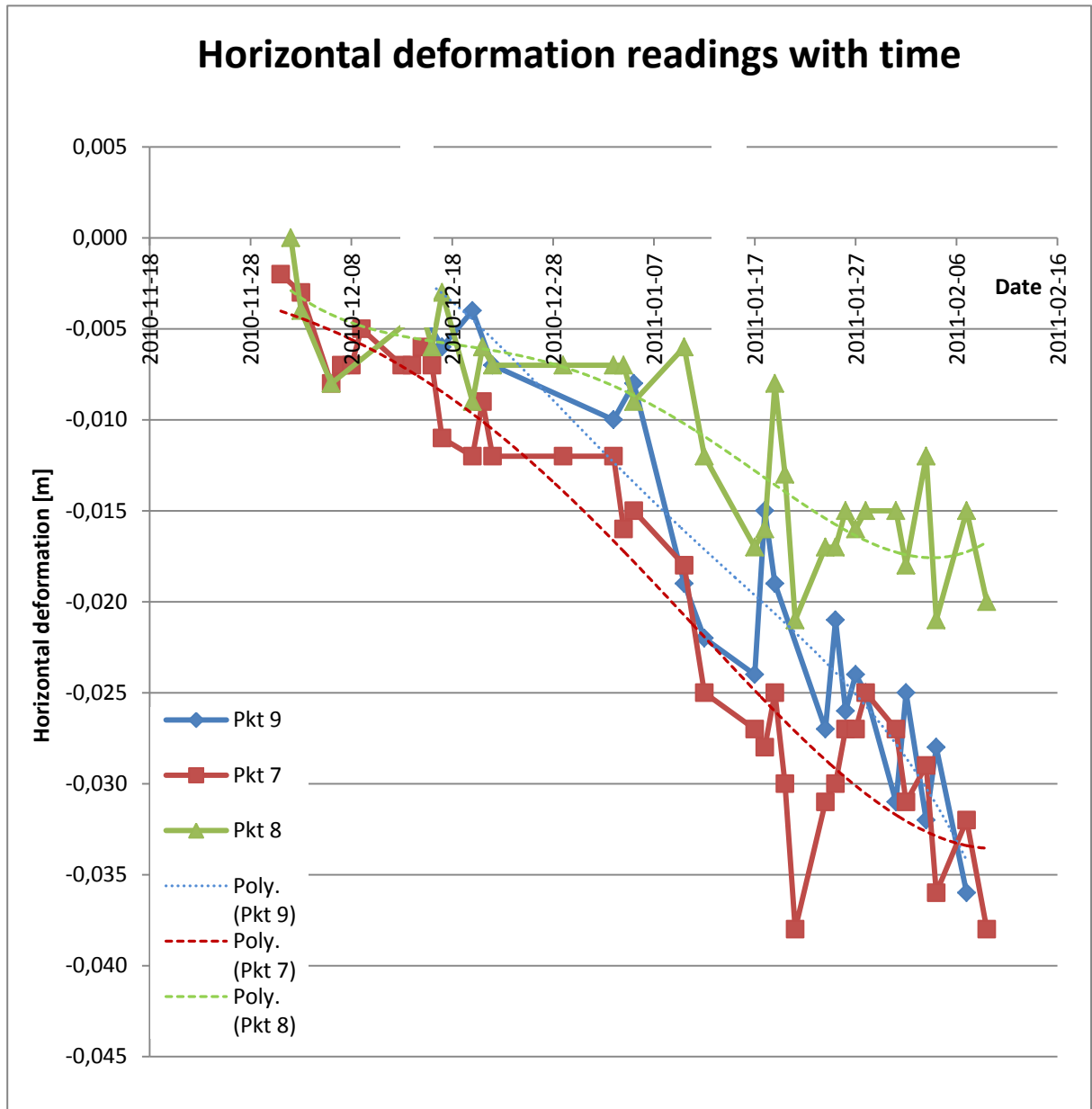


Figure 39: Horizontal deformation readings with gauges for different dates.

The measured horizontal deformation from the measurement program consisting of points at the USP and the NSP with two rows of data points is presented in Table 2.

*Table 2: Cumulative horizontal deformation at the bridge points.*

Point number	Horizontal deformation (mm)
101	42
102	40
103	43
104	42
201	29
202	30
203	32
204	11

## 4. Plaxis analysis

Once all the relevant input data from field and laboratory tests, and mathematical hand and empirical calculations are collected, the Plaxis deformation analysis proceeds. As mentioned in the theory part, the Plaxis analysis includes the input, calculation and output phases. However, in this section only the first two phases are discussed. The later phase is discussed in the result section together with the field measurements, the inclinometer readings and surface point measurements.

### 4.1 Input phase

The first step in the input phase involves creating geometry of the model which resembles to the actual conditions in section E13 where the excavation is taking place, see Figure 40.

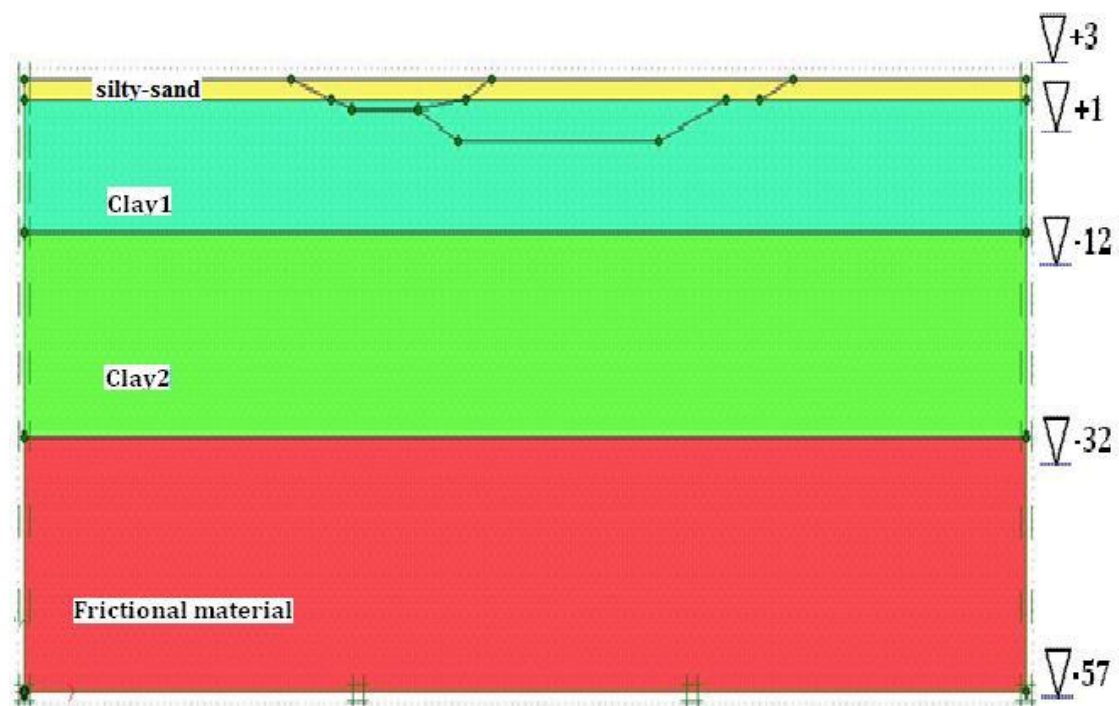


Figure 40: Geometry of model

As shown in the figure above, the geometry model consists of a section from the existing E45, which was unloaded 50 years ago, current excavation area and four different soil layers at different level modelled at a standard fixity and boundary conditions. The different soil layers have different parameter values that have to be inserted into the model at this phase. But, the type and value of soil parameters used in this project in the two soil models is discussed independently in the sub-headings below.

Once the geometry model is clearly defined and the different soil layers are assigned to their respective level, the next step is to create a triangular finite element mesh for the finite element method of Plaxis simulation. The type of mesh used in the analysis includes a medium mesh and a fine mesh. The latter mesh is used for the part where deformation measurement is of great importance, whereas the medium mesh is used for the rest of the areas that constitute the geometry model, see Figure 41.

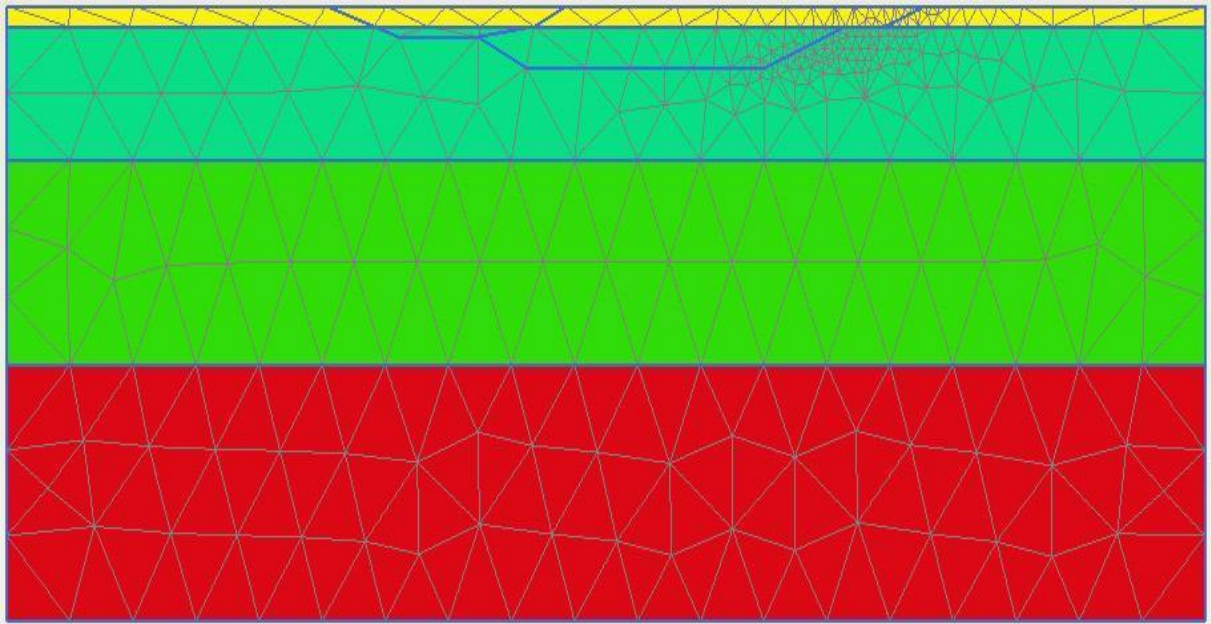


Figure 41: Generated mesh for finite element analysis.

Figure 41 shows the two types mesh that are used in this deformation analysis. The fine mesh is used in the area where the inclinometer device is in position in the actual excavation area, so that the results from the Plaxis analysis can be comparable with the inclinometer readings. This based on the fact that the finer the mesh is the better the accuracy of the calculation will be. For the rest of the area a medium mesh is used in order not to make the analysis time taking.

#### 4.1.1 Mohr coulomb

The first soil model used in this thesis is the Mohr coulomb soil model. In this model different relevant soil parameters are inserted as input value in order to satisfy the failure criterion and carry out the deformation analysis. The relevant soil parameters are obtained from field and laboratory tests and different empirical approaches, see Table 3. The analysis is based on undrained effective stress analysis (effective stiffness parameters).

Table 3: Input parameters for Mohr coulomb model

Parameter	Name	Layers				Unit
		Layer-1	layer-2	layer-3	layer-4	
soil type	soil type	silty-sand	clay-1	clay-2	frictional material	-
depth	depth	2	13	20	25	m
material model	model	Mohr-coulomb	Mohr-coulomb	Mohr-coulomb	Mohr-coulomb	-
type of material behaviour	type	drained	un-drained	un-drained	drained	-
soil unit weight above pheratic level	$\gamma_{unsat}$	18	-	-	-	$\text{KN/m}^3$
soil unit weight below pheratic level	$\gamma_{sat}$	21	16	16	21	$\text{KN/m}^3$
permeability in horizontal direction	$K_x$	1	0.000432	0.00003	1	m/day
permeability in vertical direction	$k_y$	1	0.000432	0.00003	1	m/day
young's modulus-1	$E'_{oed}$	15000	935	2335	40000	$\text{KN/m}^2$
Incremental young's modulus-1	$E'_{oed,inc}$	-	108	120	-	$\text{KN/m}^2$
young's modulus-2	$E'(5*Mo)$	15000	4360	11215	40000	$\text{KN/m}^2$
Incremental young's modulus-2	$E'(5*Mo),inc$	-	530	675	-	$\text{KN/m}^2$
young's modulus-3	$E'_{tender}$	15000	1250	4360	40000	$\text{KN/m}^2$
Incremental young's modulus-3	$E'_{tender,inc}$	-	240	258	-	$\text{KN/m}^2$
young's modulus-4	$E'_{per.}$	15000	623	9660	40000	$\text{KN/m}^2$
Incremental young's modulus-4	$E'_{per,inc}$	-	695	1600	-	$\text{KN/m}^2$
young's modulus-5	$E'_{avg}$	15000	2805	7320	40000	$\text{KN/m}^2$
Incremental young's modulus-5	$E'_{avg,inc}$	-	350	430	-	$\text{KN/m}^2$
poisson's ratio	$\nu'$	0.3	0.35	0.35	0.3	-
cohesion	$C$	0.2	13	27	0.2	$\text{KN/m}^2$
incremental cohesion	$C,inc$	-	1	1	-	$\text{KN/m}^2$
friction angle	$\phi$	36	-	-	38	$^\circ$
dilatancy angle	$\psi$	6	-	-	8	$^\circ$

Even though the analysis is based on undrained effective stress analysis, only young's modulus and poisson's ratio are used as effective parameters. This is due to not being able to get effective parameters for the other strength parameters without performing laboratory tests. Using effective values of shear strength for higher effective stresses will lead to a high shear strength compared to the undrained shear strength obtained by field and laboratory tests. The use of effective shear strength for lower effective stress states will lead to a low shear strength compared to the values of undrained shear strength obtained by field and laboratory tests see Figure 42.

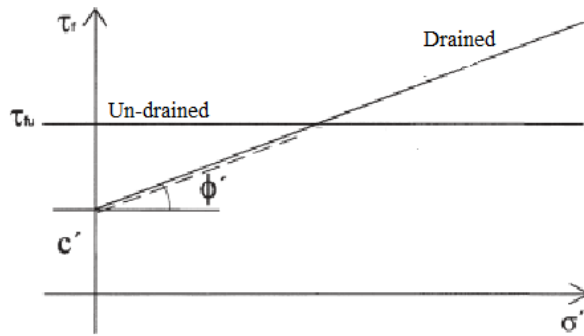


Figure 42: The relation between drained and undrained parameters for an analysis. (SGI, 2007)

However, Plaxis offers the possibility to use the original value of the strength parameters when these laboratory tests are not performed. Therefore, in this model the effective shear strength (cohesion)  $C$ , is set to be equal to the undrained shear strength  $C_u$ , and the effective friction angle  $\phi$ , is set to be equal to the friction angle  $\phi_u$ . This type of undrained analysis is called undrained B in Plaxis software. The unloading modulus, which is the main focus in this thesis, is inserted into the model in the form of oedometer modulus and four other approaches, where later on parameter analysis is performed to determine which approach will give a reasonable unloading modulus. For this soil model in parameter analysis chapter a comparison between analyses by use of effective and undrained shear strength and friction angle will be performed.

#### 4.1.2 Hardening soil

The second model used in this thesis is the Hardening soil model. In this model different kinds of soil parameters are inserted as input value in order carry out the deformation analysis in Plaxis software. The relevant soil parameters are obtained from field and laboratory tests and different empirical approaches, see Table 4. The analysis by use of hardening soil is performed by use of effective parameters.

Table 4: Input parameters for hardening soil model

Parameter	Name	Layers				Unit
		Layer-1	Layer-2	Layer-3	Layer-4	
Soil type	soil type	silty-sand	clay-1	clay-2	frictional material	-
Depth	depth	2	13	20	25	m
Material model	model	Hardening	Hardening	Hardening	Hardening	-
Type of material behaviour	type	drained	un-drained	un-drained	drained	-
Soil unit weight above pheratic level	$\gamma_{unsat}$	18	-	-	-	KN/m <sup>3</sup>
Soil unit weight below pheratic level	$\gamma_{sat}$	21	16	16	21	KN/m <sup>3</sup>
Permeability in horizontal direction	$K_x$	1	0,000432	0,00003	1	m/day
Permeability in vertical direction	$k_y$	1	0,000432	0,00003	1	m/day
$E_{oed,ref}=ML$	CRS (ML)	15000	800	800	40000	KN/m <sup>2</sup>
$E_{50,ref}=Mo,mean$	CRS (Mo,mean)	15000	5730	5780	40000	KN/m <sup>2</sup>
$E_{ur,ref}=5*Mo,mean$	CRS (5*Mo,mean)	45000	28650	28900	120000	KN/m <sup>2</sup>
$E_{50,ref}=250*C_{uk}$	250*C <sub>uk</sub>	15000	10446	10446	40000	KN/m <sup>2</sup>
$E_{ur,ref}=3*250*C_{uk}$	3*250*C <sub>uk</sub>	45000	31338	31338	120000	KN/m <sup>2</sup>
OCR	OCR	-	1,1	1,25	-	-
POP	POP	-	15	35	-	KN/m <sup>2</sup>
$K_{0,nc}$	$K_{0,nc}$	-	0,6	0,6	-	-
Poisson's ratio	$\nu_{ur}$	0,2	0,2	0,2	0,2	-
Cohesion	C	0,2	1,3	2,7	0,2	KN/m <sup>2</sup>
Incremental cohesion	$C_{inc}$	-	0,1	0,1	-	KN/m <sup>2</sup>
Friction angle	$\phi$	36	20	20	38	°
Dilatancy angle	$\psi$	6	-	-	8	°

Compared to the analysis in Mohr coulomb, the undrained analysis in hardening soil is not only performed by effective young's modulus and poisson's ratio but also effective shear strength and friction angle. This type of analysis is called undrained A in Plaxis software. This type of undrained analysis is performed because a friction angle equal to zero will lead to non stress dependent modulus which is not desirable. This type of analysis will also give a modulus which is constant with depth. Therefore, in this model the effective shear strength (cohesion)  $c$ , is set to be equal to the effective shear strength  $c'$ , and the effective friction angle  $\phi$ , is set to be equal to 20. A higher value than 20 for friction angle will give a high value of the shear strength, see figure in section 4.1.1 and this mean that obtained results are on the unsafe side.

The effective shear strength is proximally 10% of the undrained shear strength or 3% of the pre-consolidation pressure and is calculated according to the equation (24) below. (Sällfors, 2001)

$$C' = 0.1 * C_u \text{ or } 0.03 * \sigma_c \quad (24)$$

The unloading modulus, which is the main focus in this thesis, is inserted into the model in the form of oedometer modulus and one other approach, see equation (12). Later on parameter analysis is performed to determine which of these two moduli and soil model will give a reasonable unloading modulus.

## 4.2 Calculation phase

After the input of material properties and generation of the mesh in input phase of Plaxis software, initial stresses are built up in the calculation step either generating them by  $K_0$ -procedure or by gravity loading. If the layers in a profile are not horizontal, which is not the case in this project; the initial stresses have to be generated by gravity loading. This is performed by selecting Plastic and setting the Weight multiplier to 1. This type of generation of initial stresses results in unrealistic deformations and this is eliminated by setting the displacement to zero in the next calculation phase. In this project the soil layers in the current profile are horizontal and therefore the initial stresses are generated by  $K_0$ -procedure in the initial step in the calculations, by setting values of  $K_0$  and over-consolidation ratio. In this step, the ground water level has to be set and in this project it is set to 2 meters below the ground surface.

After the initial stresses have been generated the excavation of the old and the new E45 are performed. The excavation is done in four steps for the different excavation stages. In the first and the third phase plastic drained option is selected as a calculation type due to the drained behaviour of the silty sand layer. In the second and fourth phase plastic is selected as the calculation type due to the undrained behaviour of the clay. Plastic analysis is selected as calculation type due to that no time effects are considered or the deformation analysis is used to see the deformation immediately after the excavation, where no dissipation of excess pore pressure is expected to occur. The soil that is supposed to be excavated is removed by selecting defining and de-activating the soil layer. This is done in all excavation phases, see Table 5.

Table 5: Calculation phases in Plaxis.

PHASE	PHASE NUMBER	PHASE START	CALCULATION TYPE	LOADING INPUT
Initial phase	0	0		
Excavation stage 1 (Old E45)	1	0	Plastic drained	Staged construction
Excavation stage 2 (Old E45)	2	1	Plastic	Staged construction
Excavation stage 1 (New E45)	3	1	Plastic drained	Staged construction
Excavation stage 2 (New E45)	4	3	Plastic	Staged construction
Slope stability	5	4	Phi/c reduction	Incremental multipliers

Because the excavation is not an underwater excavation the ground water inside the excavation has to be removed so it will not affect the results. The removal of the water inside the excavation is performed by using a feature in Plaxis called cluster dry, see Figure 43.



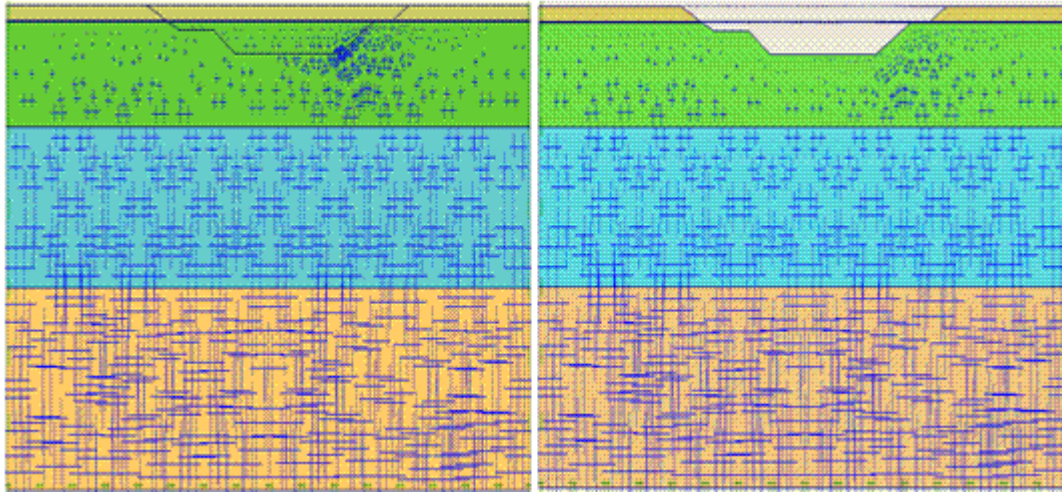


Figure 43: Dry excavation in Plaxis analysis.

In the fifth phase, see table above, the slope stability analysis is performed by an option called phi/c reduction. The idea of this calculation type is to reduce the  $c$  and  $\phi$  until the soil collapses and then the values of cohesion and friction angle are recorded. These values give at which values the soil fails and are compared to the actual shear strength and friction angle. By the comparison a safety factor  $F$  for the slope failure is obtained, see equation (25) below.

$$F = \frac{\tan \phi_{input}}{\tan \phi_{reduced}} \quad (25)$$

After the calculation step, the deformations and the stability of the slope can be evaluated in the outputs and are presented in the next chapter together with the results from field measurements.

### 4.3 Outputs

Among the different output results that can be obtained from Plaxis, such as deformations of geotechnical and structural elements, slope stability, steady pore-water pressure and development of excessive pore pressures and consolidation parameters, this thesis is concerned with horizontal displacements due to excavation. Additionally, since the excavation has taken place in short period time plastic analysis is only performed rather than consolidation analysis and all results regarding consolidation process obtained from the Plaxis simulation are therefore considered to be not relevant to this project.

The horizontal phase displacement readings are taken in form of cross section in points where the inclinometer and point measurement devices are installed in the actual excavation area, see Figure 44.

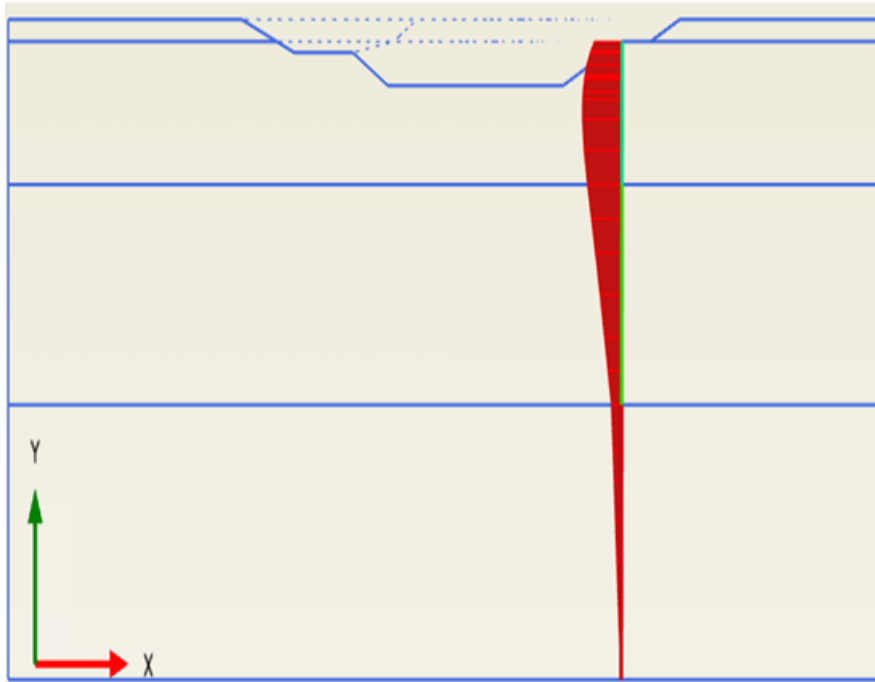


Figure 44: Horizontal displacement reading in cross section form where the inclinometer device is installed in the actual excavation area.

Readings in form of cross section are taken in order to get the relevant displacements due to the excavation and also to compare these displacements with the displacement readings from the inclinometer and point measurements. This method of comparison also helps to study the deformation properties of soft clay and is used as a method to determine which soil parameter has significant influence on deformation of soft clay.

### 4.3.1 Mohr coulomb

As stated in previous chapter, the first soil model that is used in this thesis in deformation analysis of soft clay in Plaxis is Mohr coulomb. Since the deformation properties of soil is highly dependent on the stiffness of the soil, different unloading stiffness modulus values from different empirical approaches are used as input values. The resulting deformation with the respective unloading modulus is shown in Figure 45.

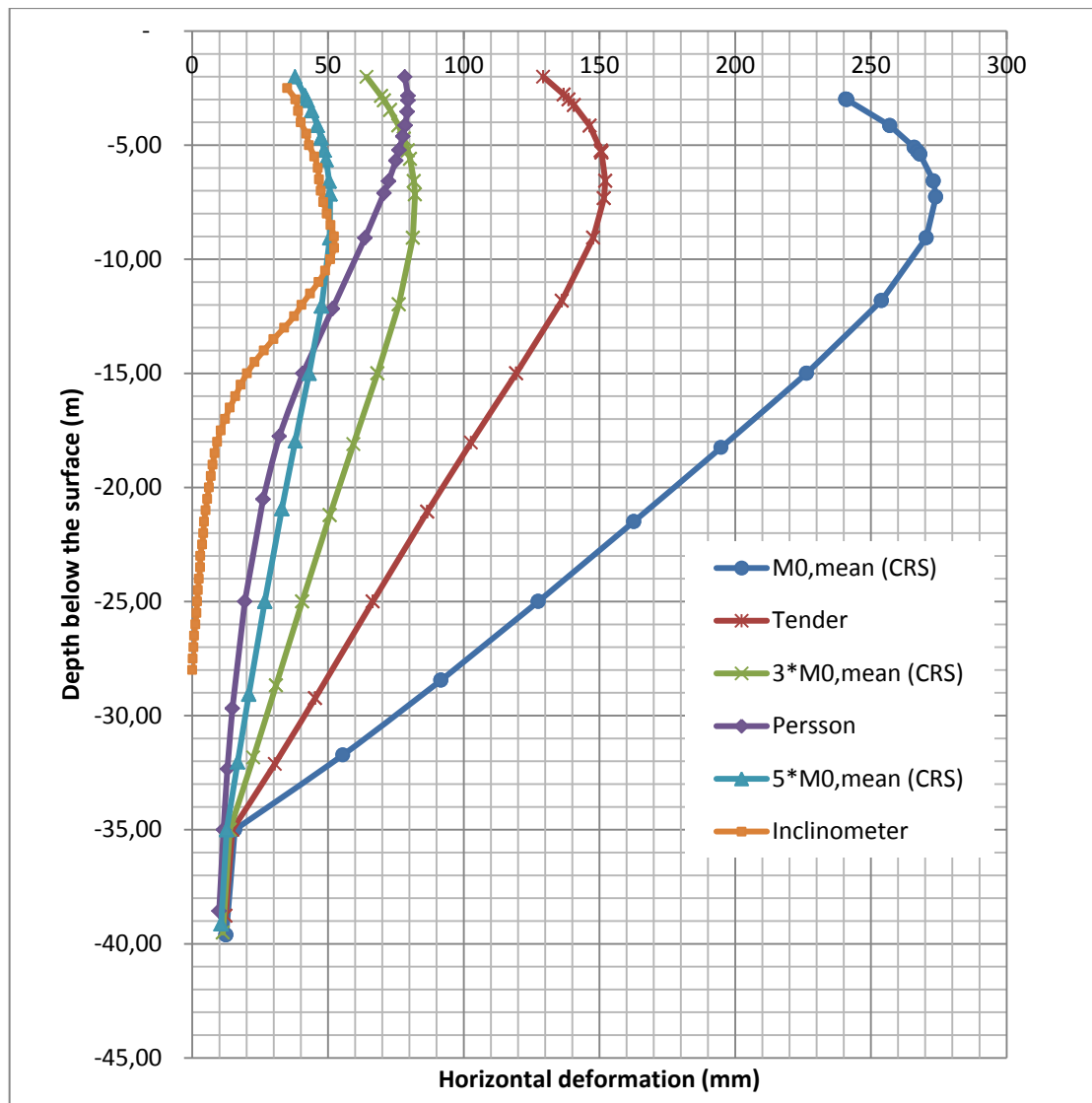


Figure 45: Horizontal deformation by using different unloading modulus in Mohr coulomb soil model plotted together with inclinometer deformation reading.

As the figure shows horizontal displacement values resulted from stiffness modulus from oedometer (CRS) test and the one that is used in the real project are considerably higher than the horizontal displacements from the inclinometer. The horizontal displacements by using stiffness modulus 3-5 times of the oedometer (CRS) and the one from Persson's empirical formula have values that are closer to the inclinometer deformation readings.

### 4.3.1 Hardening soil

The second approach used in the Plaxis is the Hardening soil model. In this model two approaches are used as input values for the reference stiffness modulus and the unloading/reloading modulus. The deformation results from Plaxis by using these two approaches are presented in Figure 46.

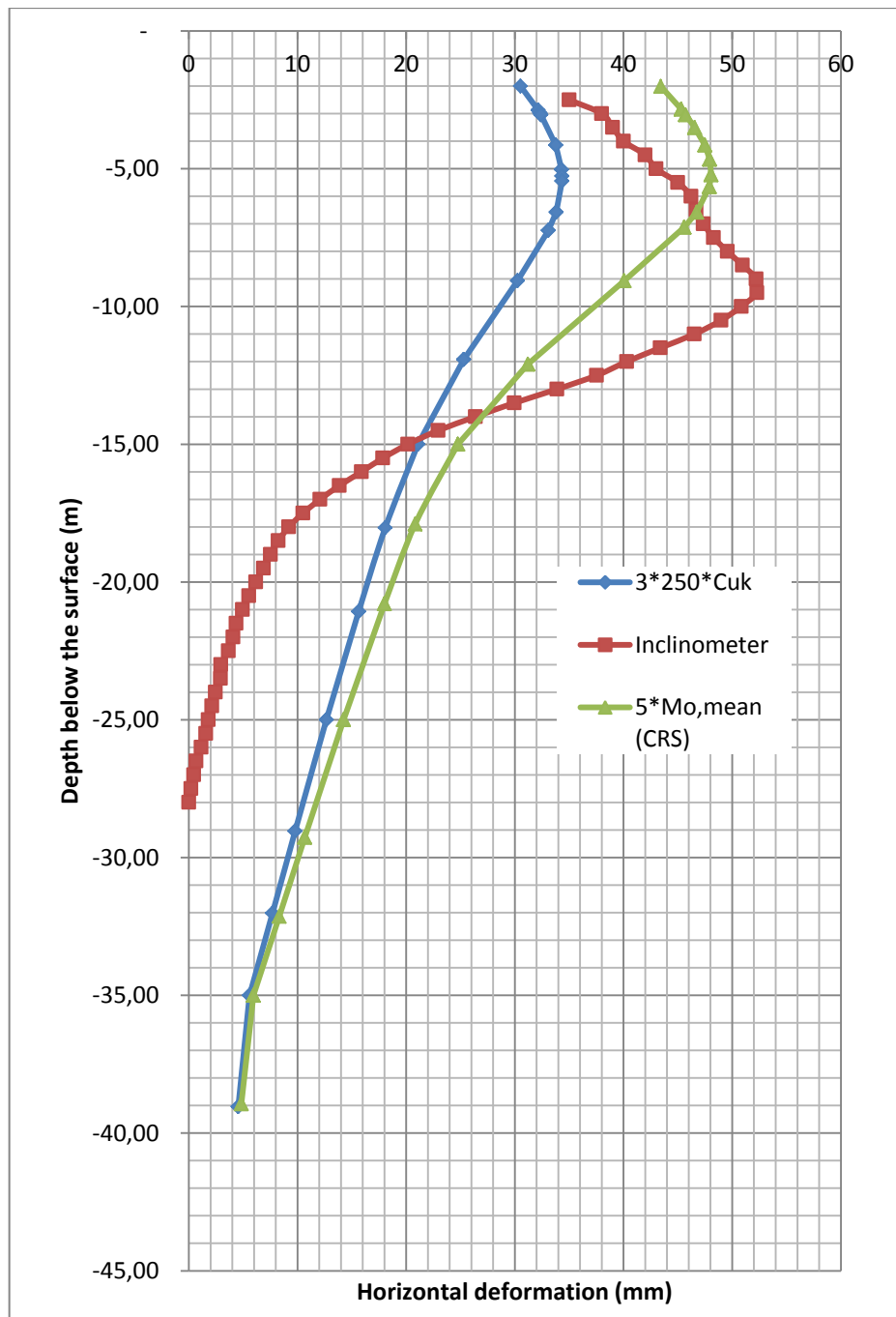


Figure 46: Horizontal deformation by using different unloading modulus in Hardening soil model plotted together with inclinometer deformation reading.

The above figure shows horizontal displacement readings from the approach that uses the unloading modulus as 5 times of  $M_0$  from the oedometer (CRS) test. The second approach uses the unloading modulus as 3 times of 250 times the undrained shear strength. For the first 15 meters of the soil layer, this approach gives lower horizontal displacements when compared to inclinometer deformation readings.

The modelled geometry of the excavation under the bridge done in Plaxis so far does not include the foundation of the bridge. Therefore, an extra model that consists of a diaphragm wall (D-Wall) installed at the inclinometer position to see how the installation of this diaphragm wall will affect the horizontal deformation that occurs due to the excavation, see Figure 47. The Diaphragm wall is installed up to a depth of

7m below the surface which is the same level with where the bridge foundation is located. The analysis is done with hardening soil model and stiffness modulus from the oedometer (CRS) is used.



Figure 47: Horizontal displacement reading when the diaphragm wall is installed at the position of the inclinometer and the installed diaphragm wall is shown highlighted in green.

The above presented diagram shows that there is a difference in value and shape of the horizontal displacement curves between the inclinometer and the modeled cases in Plaxis. The decreasing rate of the deformation curves is higher for the first 7m for the inclinometer readings than for the simulated models. This is because the foundation bridge acts like a passive force and pushes the soil back. If the foundation of bridge was not in place in the analyzed section, the deformation curve from the inclinometer would probably be similar to the simulated models in Plaxis, see Figure 48.

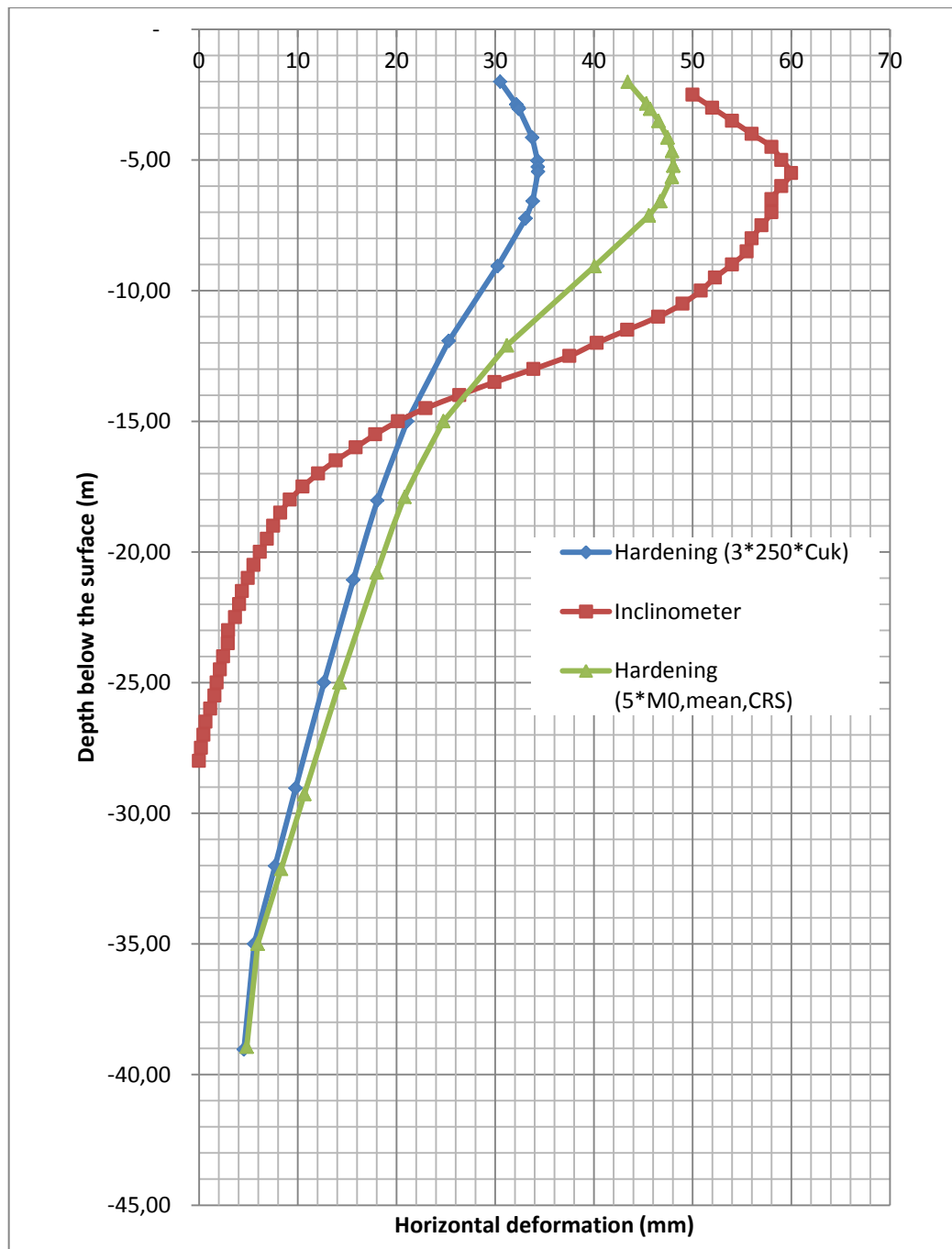


Figure 48: The deformation curve for the inclinometer without bridge foundation in the studied section compared to the modeled sections for hardening soil model.

## 5. Result comparison

In this chapter a comparison is carried out between horizontal deformations obtained from the inclinometer device and all the simulated models in Plaxis. In Figure 49 the horizontal deformation comparison between the soil models and the inclinometer device throughout the soil layer can be seen.

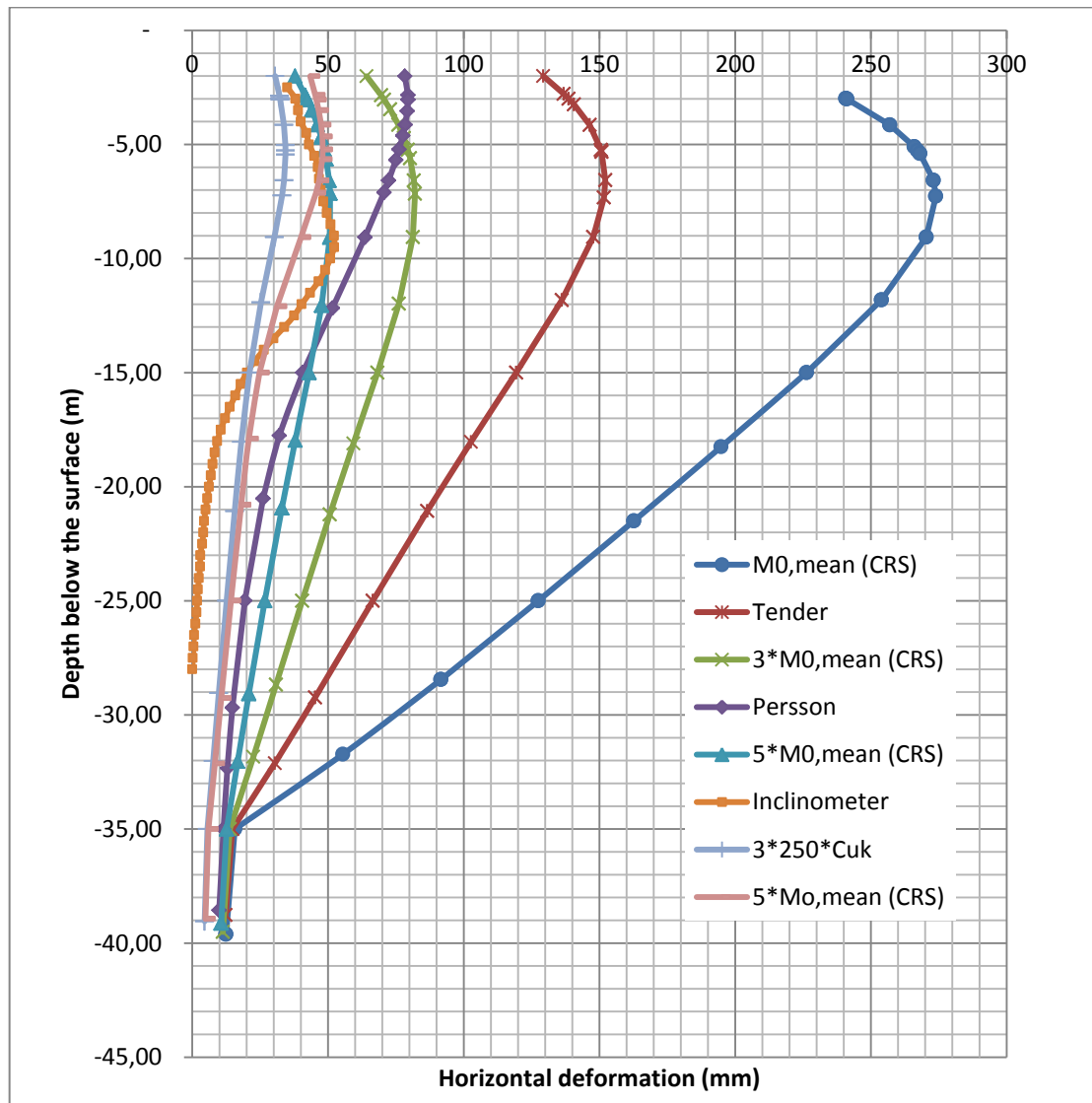


Figure 49: Horizontal deformation by using different unloading modulus in Mohr coulomb soil model (the five first names in the diagram) and Hardening soil model (the last two names in the diagram) plotted together with inclinometer deformation reading

Because of the impact of the foundation there is no possibility to make a comparison between the inclinometer readings and the simulations performed in Plaxis for the first 6-8 meters of the soil layer. Therefore the comparison is performed where the inclinometer gives largest horizontal displacements, which is around a depth of 9 meters below the ground surface. In Table 6 the horizontal deformations from the

inclinometer device for a depth of 9 meters is compared to the deformations obtained in Plaxis for the same depth by using different approaches.

Table 6: Deformation comparison between inclinometer device and outputs from Plaxis

Source	Approach	Type of soil model	Horizontal deformation (mm)
Inclinometer	Field data	Field data	52
Oedometer (CRS)	$M_0$ ,mean	Mohr Coulomb	270
Tender	$M_0=50*\sigma'_c$	Mohr Coulomb	150
Oedometer (CRS)	$3*M_0$ ,mean	Mohr Coulomb	80
Persson	See section 2.3.2	Mohr Coulomb	62
Oedometer (CRS)	$5*M_0$ ,mean	Mohr Coulomb	50
Oedometer (CRS)	$5*M_0$ ,mean	Hardening soil	40
Shear strength	$3*250*C_{uk}$	Hardening soil	30

From Table 6 it can be seen that the simulation in Mohr coulomb model by use of 5 times  $M_0$  as unloading modulus gives almost the same horizontal deformations as the measured one by the inclinometer. It can also be seen that in hardening soil model the use of unloading modulus as 5 times  $M_0$  from CRS test gives deformations that are similar to the inclinometer readings.

In Table 7 the horizontal deformations from the point measurements in point 9 are compared to the surface deformations obtained in Plaxis by using different approaches. This point is selected because of its closer distance to the simulated section in Plaxis.

Table 7: Deformation comparison between point measurements and outputs from Plaxis

Source	Approach	Type of soil model	Horizontal deformation, point 9 (mm)
Gauges (point measurement)	Field data	Field data	35
Oedometer (CRS)	$M_0$ ,mean	Mohr Coulomb	139
Tender	$M_0=50*\sigma'_c$	Mohr Coulomb	78
Oedometer (CRS)	$3*M_0$ ,mean	Mohr Coulomb	42
Persson	See section 2.3.2	Mohr Coulomb	41
Oedometer (CRS)	$5*M_0$ ,mean	Mohr Coulomb	25
Oedometer (CRS)	$5*M_0$ ,mean	Hardening soil	21
Shear strength	$3*250*C_{uk}$	Hardening soil	14



## 6. Parameter analysis

In order to evaluate the impact of some input parameters on the deformation analysis a parameter analysis is performed. In this analysis three important parameters are analysed by changing the value of them according to typical values for the specific parameter. Bulk density of the clay, geometry of the excavation model, and the modulus of the clay are the parameters evaluated in this thesis.

The bulk density of clay varies between 15-17 kN/m<sup>3</sup> and in this thesis a value of 16 kN/m<sup>3</sup> was used for the entire clay layer. To see the impact of change of the value of the density on the horizontal deformations, the density of the clay is changed to 15 and 17 kN/m<sup>3</sup> respectively. The analysis shows that using a density value smaller than 16 kN/m<sup>3</sup> in hardening soil model gives higher horizontal displacements and lower horizontal displacements when using a higher density value. This is due to the fact that hardening soil model takes into account change of stiffness of soil with change of stresses. However, this is not the case in Mohr coulomb soil model.

The geometry of the excavation has also an impact on the results obtained from Plaxis. The parameters in the geometry such as the angle of the slope, has a direct effect on the deformation results. A steeper slope will lead to higher horizontal displacements and vice versa. Therefore, increasing the accuracy of the geometry model of the excavation area in Plaxis will give better and realistic results.

The results from simulated models in Plaxis using different empirical approaches to determine the unloading stiffness modulus of the soil gives a clear picture of the importance of the modulus on the deformations.

The results obtained by using Mohr-coulomb soil model show that the modulus used in the tender document as unloading modulus leads to displacements that are higher than what they are in reality. This is also the case when using the  $M_0$  evaluated from a CRS-test as unloading modulus. This means that these moduli are small and indicates that the soil is not stiff enough in Plaxis compared to what it is in reality.

To obtain deformations results as realistic as possible there is a need of using accurate stiffness parameters like the unloading modulus. Table 8 shows what value to use as the unloading modulus in Mohr-coulomb when using the different empirical approaches.

Table 8: Unloading modulus in Mohr-coulomb soil model

Approach	Unloading modulus
CRS ( $M_0$ )	$(3-5)*M_0$
$M_{tender}$	$(2-3)*50*\sigma'_c =$ $(100-150)*\sigma'_c$

The results obtained from Hardening soil model show that using 3 times 250 times the undrained shear strength as the unloading modulus leads to horizontal displacements that are lower than what they are in reality. Therefore a factor of two is better to use

instead of three in Plaxis to determine the unloading modulus. However, when using the 5 times  $M_0$  evaluated from a CRS-test as the unloading modulus the horizontal displacements are almost the same as the inclinometer readings for the first 15 meters of the clay layer. Table 9 shows what value to use as secant modulus in Hardening soil model and what factor to use to determine the unloading modulus.

Table 9: Unloading modulus in Hardening soil model

<b>Approach</b>	<b>Secant modulus</b>	<b>Unloading modulus</b>
<i>CRS (<math>M_0</math>)</i>	$E_{50} = M_0$	$E_{ur} = 5 * E_{50}$
<i><math>M_{cuk}</math></i>	$E_{50} = 250 * C_{uk}$	$E_{ur} = 2 * E_{50}$
<i><math>M_{tender}</math></i>	$E_{50} = 50 * \sigma'_c$	$E_{ur} = 2 * 50 * \sigma'_c$ $= 100 * \sigma'_c$

## 7. Conclusion and discussion

After performing two dimensional Plaxis deformation analysis of soft clay due to unloading by using two different soil models, Mohr coulomb and Hardening soil model, and by using around six empirical approaches to determine the unloading soil modulus, it has been seen that the soil stiffness modulus from the empirical approach  $3-5 * M_0$ , more specifically,  $5 * M_0$  gives better and realistic result when compared with the results from field inclinometer and point measurement readings. It was expected that the horizontal displacements obtained from Plaxis must be lower than the displacement readings obtained from the inclinometer. This is due to the fact that the horizontal displacement readings from Plaxis are available only in horizontal direction where as the readings from the inclinometer are available in the form of horizontal (x & y) direction and as a resultant of the two directions, and the displacement readings from Plaxis are only compared with the resultant displacement readings from inclinometer. Among the different empirical approaches that is used to estimate the soil stiffness modulus,  $5 * M_0$  has been seen to satisfy the above condition.

According to the parameter analysis, changing the stiffness modulus and the density of the soil and the geometry of the model in Plaxis affects the deformation analysis. Special care must be taken when choosing the value and conditions of these parameters, specially, the stiffness modulus of soil, since in this thesis it has been noted that the deformation of soft clay is directly related to its corresponding stiffness. Additionally, the results from Plaxis simulation and field measurements show that it is possible to use the empirical relation  $3-5 * M_0$  and 2-3 times of the other empirical approaches  $250 * C_{uk}$  and  $50 * \sigma'_c$  respectively, where laboratory tests are not conducted to determine the unloading modulus of soft clay.

It is difficult to analyse and model the deformation properties of soft soil by using different empirical approaches, and with computer software simulation, since the deformation properties of soft soil in reality tend to be different from the empirical approaches and computer software simulations. Moreover, the different soil parameters and other conditions that are obtained from the field investigations and laboratory tests must be as perfect as possible in order to get a better and realistic result.

To sum up, in deformation analysis of soft soil, it will be a good choice to choose the approach that gives a lower modulus among the different approaches to determine the soil stiffness modulus when dealing with big geotechnical projects where any kind of risk or uncertainty of safety is not acceptable. In contrast to this, it will be a good choice to choose the approach that gives a higher soil modulus when dealing with geotechnical projects that economy of the project is of great importance and if all soil parameters and other conditions are determined as perfect as possible.

## 8. Recommendations

In this master's thesis, the deformation analysis soft clay due to excavation is performed through the help of Plaxis simulation. As stated earlier, it is a bit complex to catch and model the real behaviour of soft soil due to unloading in Plaxis simulation. Therefore, increasing the accuracy of the investigation of important soil parameters and other conditions will not only make the Plaxis simulation less complicated, but also affects the results from the simulation towards favourable direction.

The first suggestion is concerned with the soil stiffness modulus which is the aim of this thesis. Normally, the unloading modulus of soft clay is determined by performing unloading and reloading test in the oedometer laboratory test. However, this test is not performed in this thesis. By performing this test a good value of the unloading modulus can be attained, and this value can be compared with the empirical approaches and a further better value can be attained. Additionally, better and realistic results that resemble the deformation behaviour in reality from Plaxis deformation simulation can be expected.

The other soil parameter that needs further investigation is shear strength. The undrained shear strength of the clay determined from the field and laboratory tests has failed to satisfy Hansbo's relation being lower than the limit value leading to make a conclusion that further investigation shall be carry out in order to get a reasonable value.

Last but not least, further investigations on parameters and other conditions that affect the deformation analysis of soft clay like liquid limit, density and swelling parameters of the clay, field deformation measurements and influence of structural elements on the deformation near excavation area shall be carried out in order to increase the accuracy of the deformation analysis and decrease the probability of occurrence of errors.

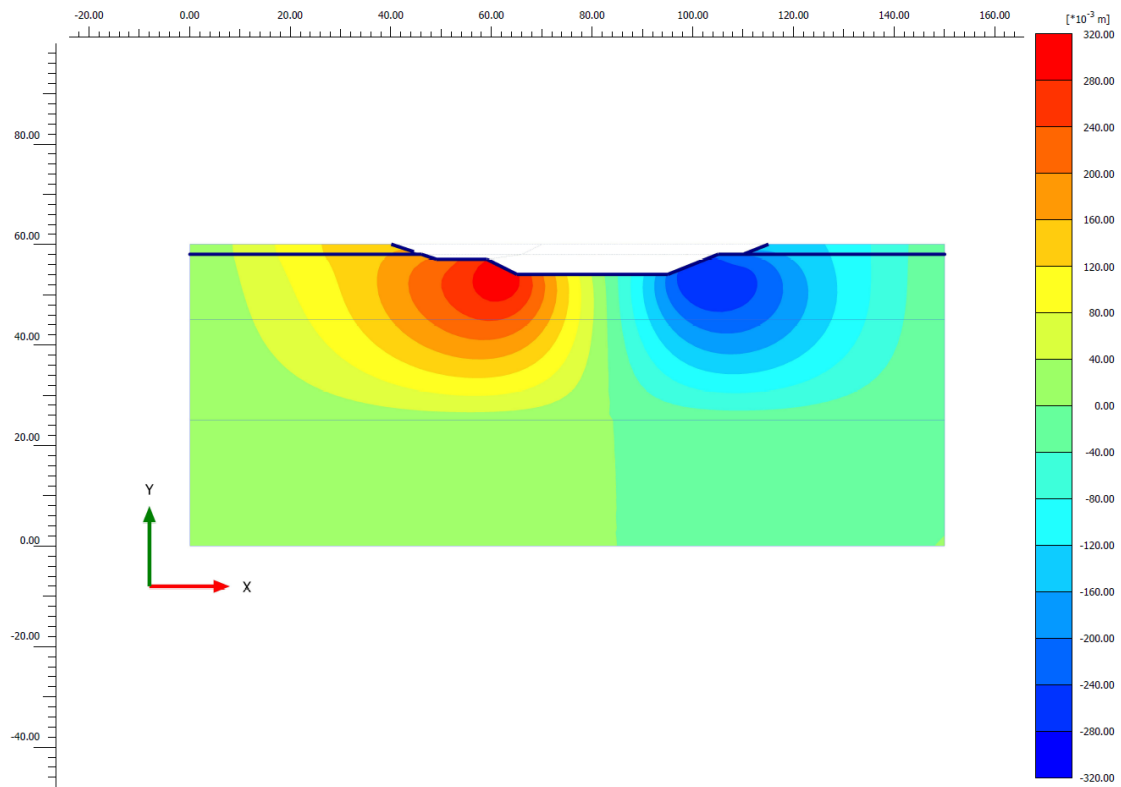
## References

- Briaud, J.L. (2010): *Introduction to soil moduli*. Department of Civil Engineering, A&M University, College Station, Texas, USA, 2010. Available at [http://www.intelligentcompaction.com/downloads/IC\\_RelatedDocs/SoilCmpct\\_BR\\_IAUD\\_Introduction%20to%20Soil%20Moduli.pdf](http://www.intelligentcompaction.com/downloads/IC_RelatedDocs/SoilCmpct_BR_IAUD_Introduction%20to%20Soil%20Moduli.pdf) [Accessed 2011-02-15]
- Brinkgreve, R.B.J. et al (2010): *Plaxis manuals, 2D-version 10*. Delft University of Technology, The Netherlands.
- Brouwer, J.J.M. (2007): *In-situ soil testing*. Delft University of Technology, {The Netherlands}, {2007}, 144 pp. Available at : <http://www.conepenetration.com> [Accessed 2011-02-13]
- Eniro.se. (2011). Available at : [www.Eniro.se](http://www.Eniro.se) [Accessed 2011-05-02]
- GEOTip (2011): *Consistency index*, Publisher, {Germany}. Available at: <http://geotip.igt.ethz.ch> [Accessed 2011-05-02]
- Houlsby, G.T. (1982): *Theoretical analysis of the fall cone test*. Available at <http://www-civil.eng.ox.ac.uk/people/gth/j/j3.pdf>[Accessed 2011-02-27]
- Kullingsjö, A. (2007): *Effects of deep excavations in soft clay on the immediate surroundings*. Ph.D. Thesis. Department of Civil and environmental Engineering, Chalmers University of Technology, Göteborg, Sweden, 2007, 334 pp.
- Larsson, R. (2008): *Jords egenskaper*. Statens geotekniska institute (Swedish geotechnical institute), Information 1, Linköping, {Sweden}, {2008}, 58 pp.
- Persson, J. (2004): *The unloading modulus of soft clay: A field and laboratory study*. Licentiate thesis. Department of Geo Engineering, Chalmers University of Technology, Göteborg, Sweden, 2004, 127 pp.
- SGI (2007): *Deponiers stabilitet*, Information 19, Linköping, {Sweden}, {2007}, 46 pp.
- SGI (1995): *Geotechnical Properties of Clay at Elevated Temperature*, Report 47, Linköping, {Sweden}, {1995}, 69 pp.

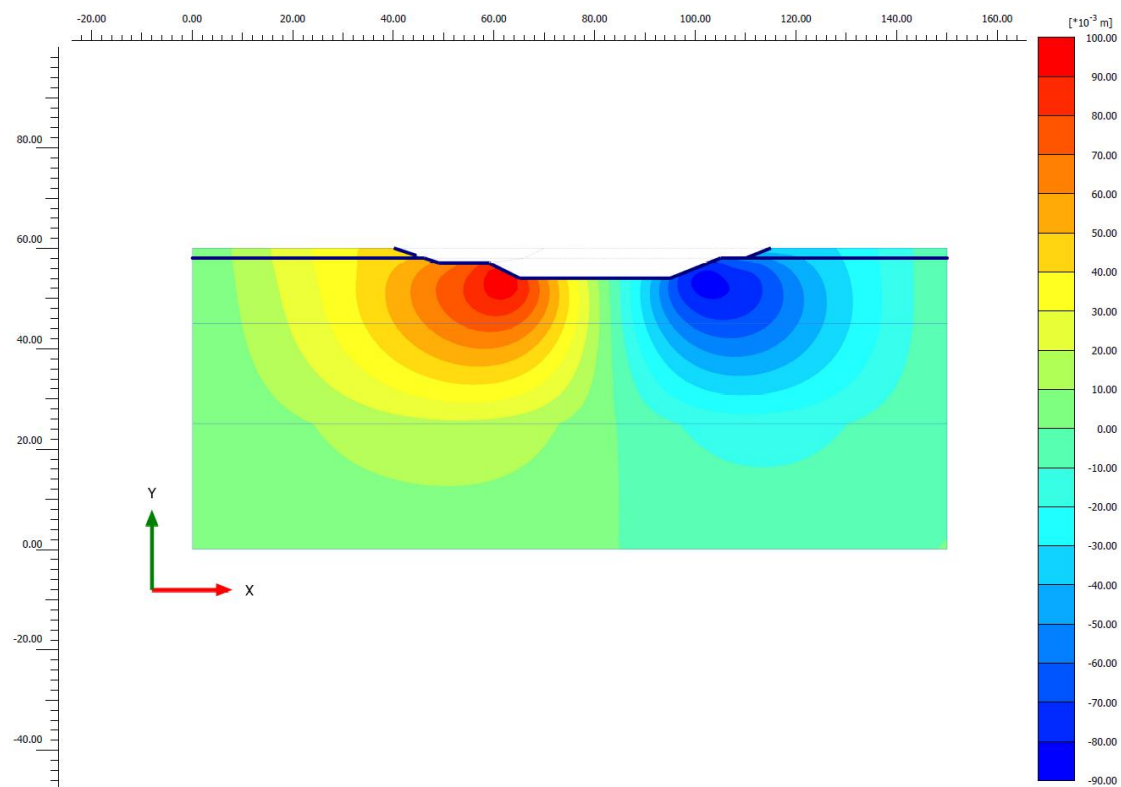
Sällfors, G. (2001): *Jordmateriallära-Jordmekanik*. 3:rd edition. Chalmers University of Technology, Göteborg, {Sweden}, {2001}, 141 pp.

The comet group program (2011), University Corporation for Atmospheric Research, Colorado, {USA}, {2011}, Available at: [www.meted.ucar.edu](http://www.meted.ucar.edu) [Accessed 2011-02-13]

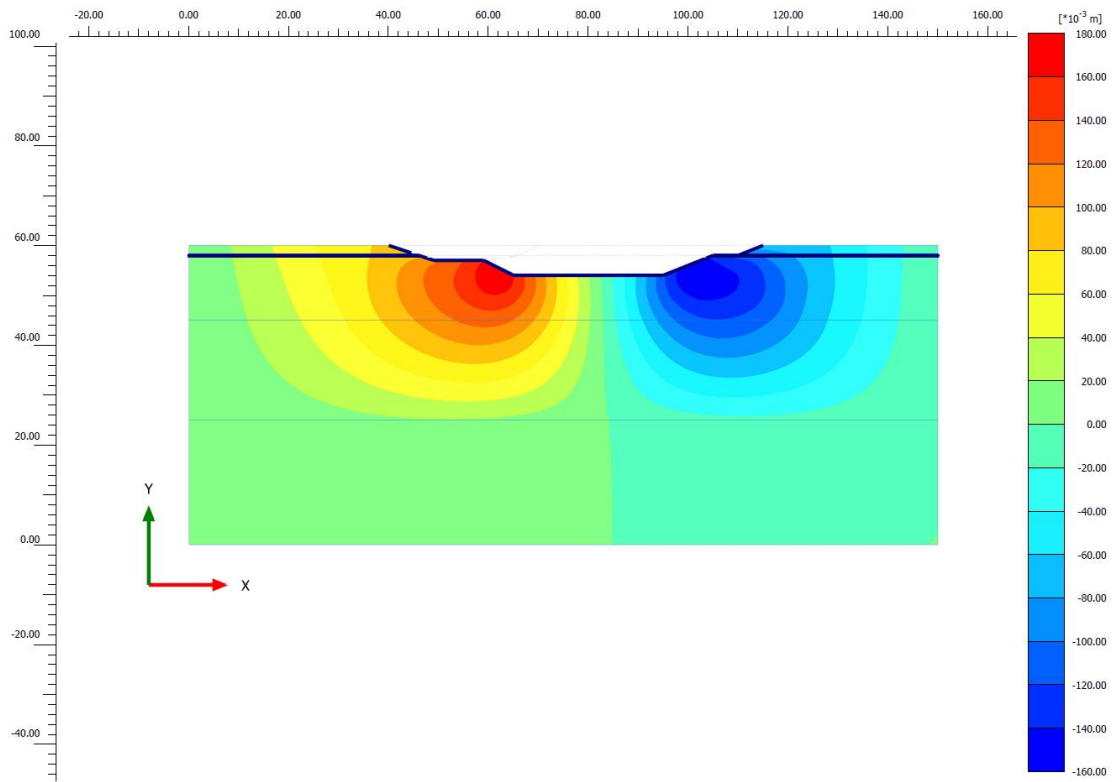
# Appendices



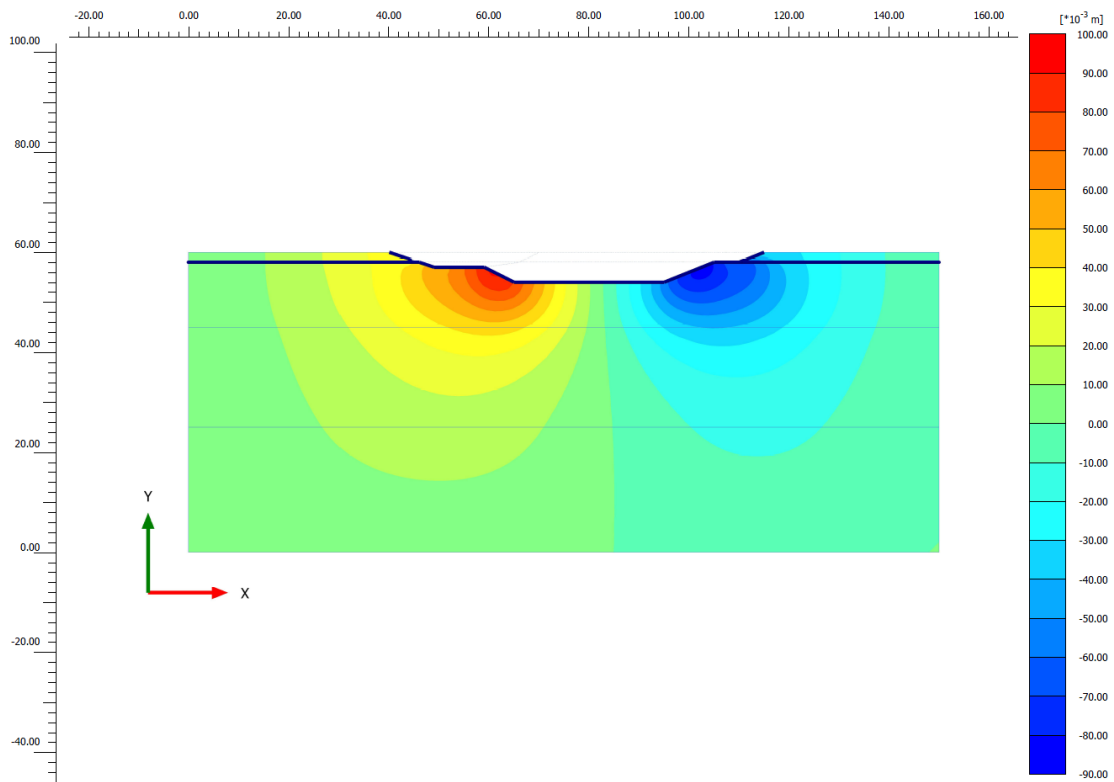
A)  $M_u = M_{0,mean} \text{ (CRS)}$ , Mohr Coulomb soil model



B)  $M_u = 3 * M_{0,mean} \text{ (CRS)}$ , Mohr Coulomb soil model

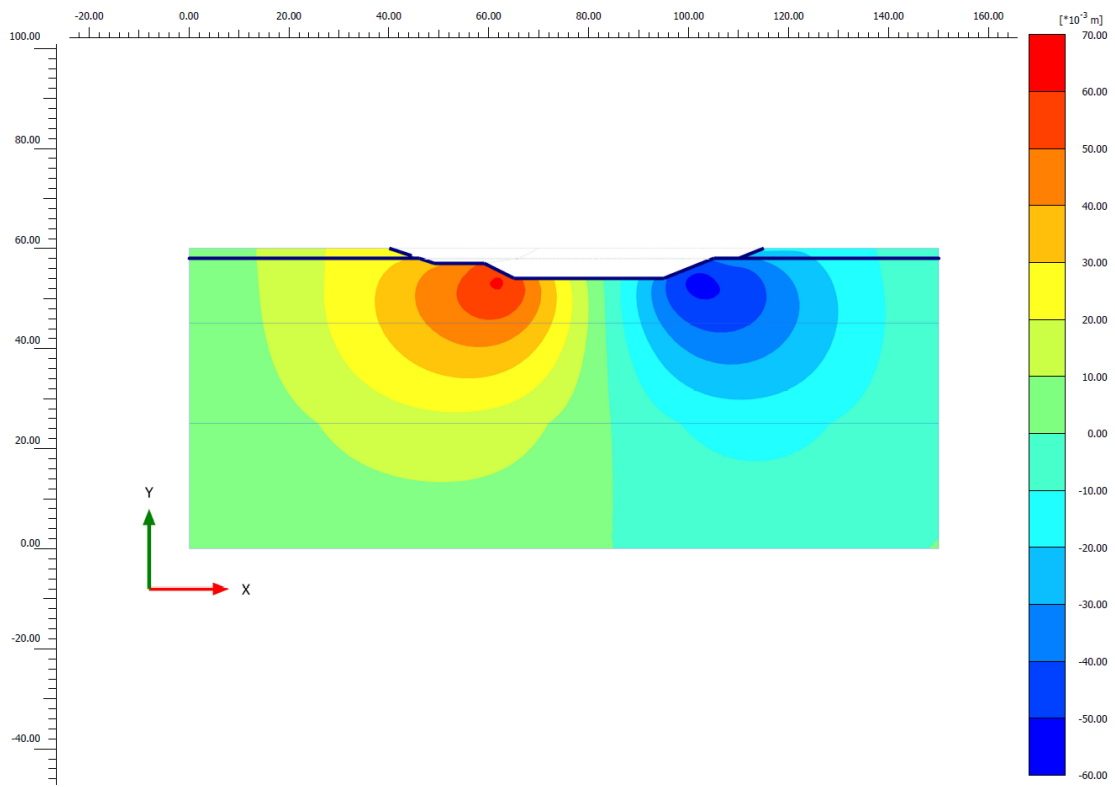


C)  $M_u = 50 \cdot \sigma_c$  (Tender), Mohr Coulomb soil model

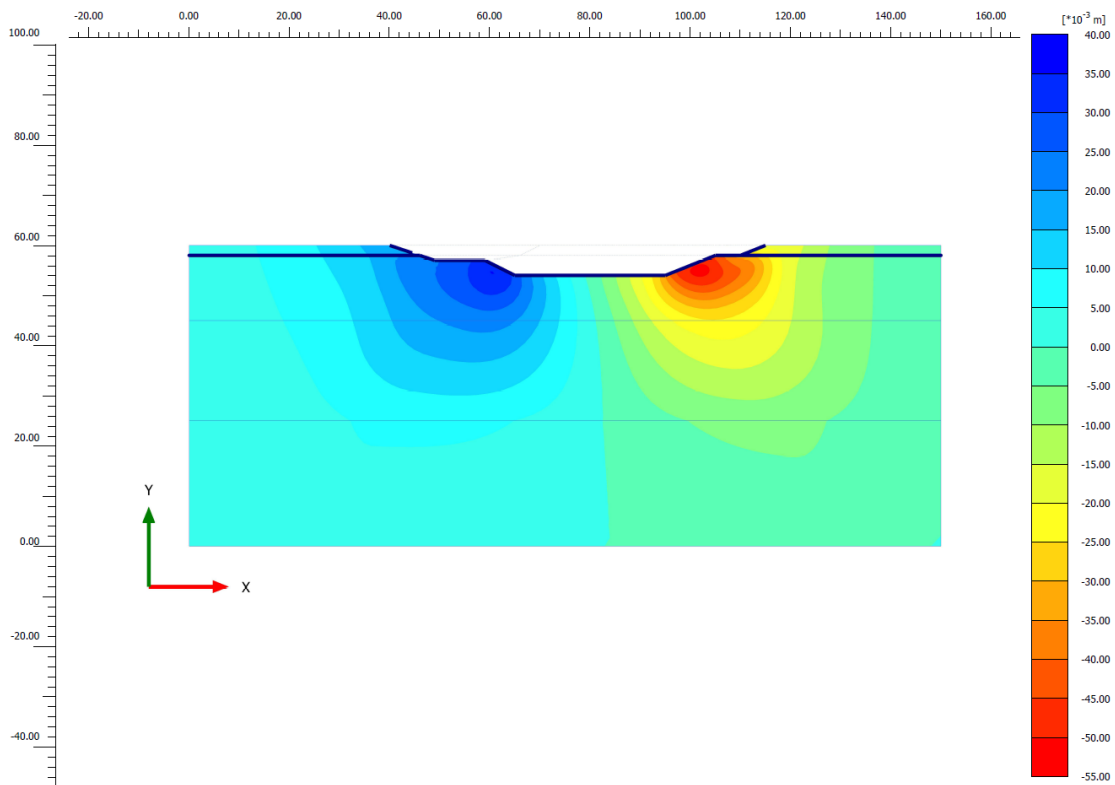


D)  $M_u =$  Persson's approach, Mohr Coulomb soil model

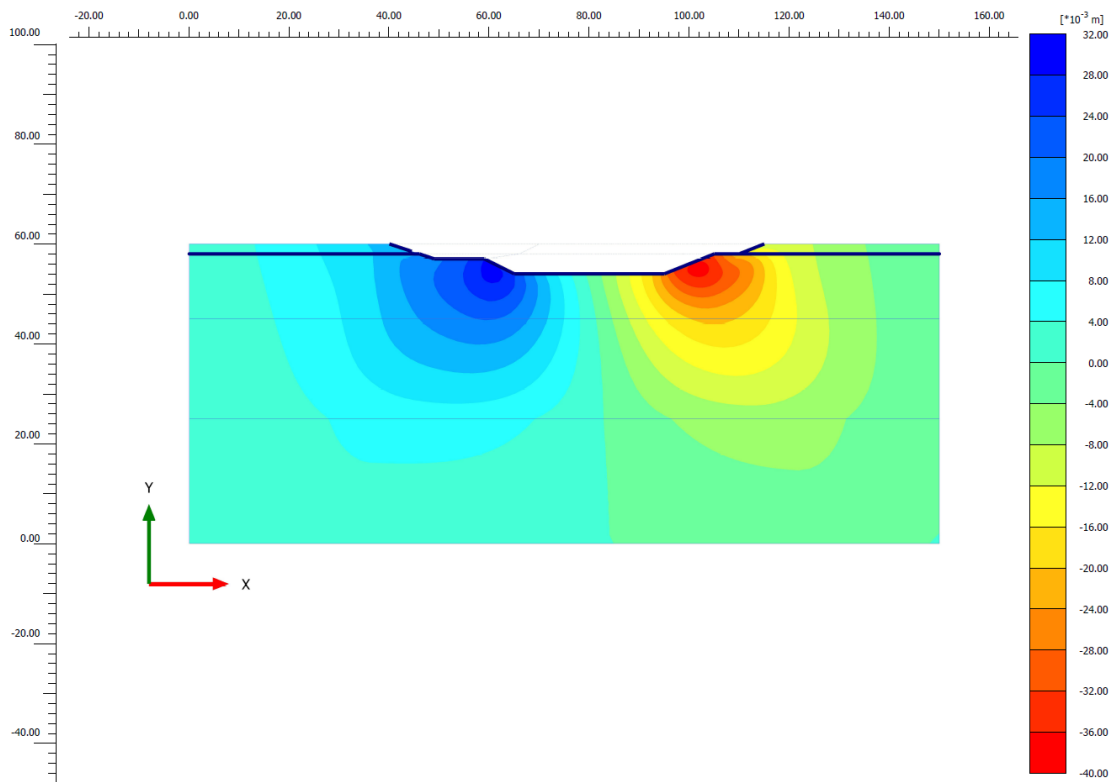




E)  $M_u=5*M_{0,mean}$  (CRS), Mohr Coulomb soil model



F)  $M_u=5*M_{0,mean}$  (CRS), Hardening soil model



G)  $M_v=3*250*C_{uk}$  Hardening soil model